Miocene faulting in the southwestern Sierra Madre Occidental, Nayarit, Mexico: kinematics and segmentation during the initial rifting of the southern Gulf of California

Jose Duque-Trujillo[1,*], Luca Ferrari[1], Gianluca Norini[2], and Margarita López-Martínez[3]

[1] *Centro de Geociencias, Universidad Nacional Autónoma de México, Campus Juriquilla, Blvd. Juriquilla 3001, 76230 Querétaro, Qro., Mexico.*
[2] *Istituto per la Dinamica dei Processi Ambientali – Sezione di Milano, Consiglio Nazionale delle Ricerche, via Pasubio 5, 24044 Dalmine (BG), Italy.*
[3] *División de Ciencias de la Tierra, Centro de Investigación Científica y de Educación Superior de Ensenada (CICESE), Carretera Ensenada-Tijuana No. 3918, 22860 Ensenada, B.C., Mexico.*
** jduquetr@gmail.com*

ABSTRACT

Crustal stretching affecting western Mexico during the Neogene, and its relationship with the opening of the Gulf of California, has been widely studied and discussed for several decades. Nevertheless, the timing and kinematics of the opening is a matter of debate. Most authors essentially agree in considering the rupture of the lithosphere around the Gulf of California, as a fast process that began at ~12.5 Ma and became successful in the early Pliocene, when new oceanic crust began to form in the southern Gulf of California. However, recent studies demonstrated that the crustal stretching processes leading to the Gulf opening began in Late Oligocene as a wide rift, which subsequently focused into the present Gulf area in the early Miocene, accompanied by a slight change in the direction of extension. Eventually, after subduction ceased, highly oblique transtensional deformation broke the previously extended lithosphere.

In this work we present a structural study of the kinematics and time of faulting, and of mafic dikes along three transects in the southern Sierra Madre Occidental, along the southeastern margin of the Gulf. We found that the deformation associated with the beginning of the Gulf of California rifting can be grouped in three sets: 1) normal faults formed during a first phase of deformation, beginning at ~24 Ma, characterized by E-W extension; 2) normal faults and dikes formed between ~20 and 11 Ma, associated with a second deformation phase, with ENE-WSW extension; 3) E-W to NE-SW oblique slip and strike-slip faults and dikes, associated with rift accommodation zones that segment the Gulf of California rift. No significant deformation occurred in the study area after 11 Ma, time at which the extension focused in the present Gulf region. The kinematics of faulting in the study area excludes that significant oblique or lateral deformation might have occurred during the initial phase of rifting in the southern Gulf of California, coincident with the last phase of subduction.

Key words: Sierra Madre Occidental; extensional tectonics; kinematics; Miocene; Gulf of California; Mexico.

RESUMEN

El proceso de extensión cortical de la margen occidental de México durante el Neógeno y su relación con la apertura del Golfo de California ha sido estudiado y discutido por varias décadas. Sin embargo la temporalidad y la cinemática de esta apertura son temas todavía debatidos. La mayoría de los autores concuerdan en que la ruptura de la litósfera en el Golfo de California fue un proceso rápido que inició a los ~12.5 Ma, para culminar al principio del Plioceno, cuando comienza el proceso de oceanización en las cuencas de la parte sur del Golfo. Sin embargo, trabajos recientes han demostrado que el proceso de extensión cortical que llevó a la apertura del Golfo comenzó desde el Oligoceno tardío a manera de un rift amplio, para posteriormente focalizarse en la zona del futuro Golfo de California en el Mioceno inferior, acompañado de un ligero cambio en el dirección de extensión. Finalmente, después del termino de la subducción, la deformación transtensional fuertemente oblicua terminó de romper la franja de litósfera previamente extendida.

En este trabajo se presenta un estudio estructural de la cinemática y la temporalidad del fallamiento, y de los diques máficos a lo largo de tres transectos en la zona suroccidental de la Sierra Madre Occidental, la cual constituye la margen suroriental del Golfo. Los resultados indican que las estructuras observadas se pueden agrupar en tres familias: 1) fallas normales asociadas a una primera fase de deformación que comienza hacia los ~24 Ma, y se caracteriza por una extensión con dirección E-W; 2) fallas normales y diques, entre ~20 y 11 Ma, asociados a una extensión orientada en dirección ENE-WSW, ortogonal al eje del Golfo de California; 3) fallas oblicuas y laterales, y diques de dirección E-W a NE-SW que se asocian a zonas de acomodo que segmentan transversalmente al rift del Golfo de California. Cabe mencionar que no hay deformación significativa después de los 11 Ma, tiempo en que la extensión se concentra en la región actualmente ocupada por el Golfo. La cinemática asociada al fallamiento observado indica movimientos dominantemente de tipo normal, lo cual excluye la posibilidad de que se hayan acomodado movimientos oblicuos o laterales durante las primeras etapas de apertura del Golfo de California, ocurridas durante la fase final de la subducción.

Palabras clave: Sierra Madre Occidental; tectónica extensional; cinemática; Mioceno; Golfo de California; México.

Duque-Trujillo, J., Ferrari, L., Norini, G., López-Martínez, M., 2014, Miocene faulting in the southwestern Sierra Madre Occidental, Nayarit, Mexico: kinematics and segmentation of the initial rifting in the southern Gulf of California: Revista Mexicana de Ciencias Geológicas, v. 31, núm. 3, p. 283-302.

INTRODUCTION

The age and kinematics of the extensional deformation that led to the formation of the Gulf of California is a matter of debate. Early studies proposed that in the middle to late Miocene the lithosphere in the area, called "proto-Gulf", was rheologically weakened by the previous (early/middle Miocene) arc-volcanism, a feature that was subsequently exploited by strike-slip and extensional faulting that led to the Gulf of California opening (Karig and Jensky, 1972; Umhoefer, 2011). Later, Stock and Hodges (1989) proposed that the initial phase of opening of the Gulf of California began in late Miocene (*ca.* 12 Ma) and was partitioned into strike-slip motion along the Tosco-Abreojos fault system, west of Baja California, and orthogonal extension (WSW-ENE) in a broadly NNW belt along the main Gulf axis. Subsequently, beginning near the end of the late Miocene (*ca.* 6 Ma), the main deformation focused east of Baja California and transtensional deformation produced the final rupture of the lithosphere and the oblique opening of new oceanic basins.

Further studies in Sonora and Baja California questioned the initial partitioning of deformation proposed by Stock and Hodges (1989) and led to alternative models, which state that the deformation inside the Gulf was characterized by right-lateral transtension since ~12.5 Ma, with a smaller component of right lateral motion accommodated west of Baja California along the Tosco-Abreojos fault system (*e.g.* Gans, 1997; Fletcher *et al.*, 2007). Recently, Bennett *et al.* (2013) proposed a hybrid model of rifting, in which the deformation along the northern Gulf was focused on a right-lateral shear zone, which later evolved into a transtensional plate limit, forming the Gulf of California rift (Bennett, *et al.*, 2013; Bennett and Oskin, 2014). All these models, however, agree on placing the initiation of the regional dextral-oblique Pacific-North America relative plate motion at ~12.5 Ma, when the subduction of the Farallon plate remnants under North America ceased and Baja California began to be transferred to the Pacific Plate (Atwater and Stock, 1998).

More recent studies of the regional geology of northern Nayarit and Sinaloa demonstrated that extensional faulting began much earlier than the end of subduction at ~12.5 Ma (Ferrari *et al.*, 2013). These authors shown that extension in the south-western part of the Sierra Madre Occidental (SMO) is as old as late Oligocene to early Miocene and likely controlled the style and composition of volcanism. Based on the reconstruction of the paleo-position of Baja California, Ferrari *et al.* (2013) also proposed that the early extension (24 to 18 Ma) in northern Nayarit and southern Sinaloa was almost orthogonal to the margin of the southern Gulf (southern Sinaloa and Nayarit) (see their fig. 15) predicting a minor component of right lateral motion, if any, in this region. This deformation is very similar to that of Sonora, where a 250 km wide belt in the western SMO was extended between late Oligocene and middle Miocene (McDowell *et al.*, 1997; González-León *et al.*, 2000; Vega-Granillo and Calmus, 2003; Nourse *et al.*, 1994; Wong *et al.*, 2010; Murray *et al.*, 2013). Following Ferrari *et al.* (2013), in this work we consider that the Gulf of California rift is the result of a long period of crustal thinning that began in the late Oligocene, and became highly oblique once Baja California started moving with the Pacific plate after the end of subduction (*ca.* 12.5 Ma).

Here, we present a geologic and structural study of the southwestern part of the SMO in Nayarit, which constrains the kinematics of the early deformation in the southeastern flank of the Gulf of California rift. We describe the stratigraphy, as well as the geometry, kinematics and age of faulting along three transects that run almost orthogonal to the main fault systems of this part of the SMO. We found that faulting and volcanism occurred concurrently during the early Miocene under an E-W to ENE-WSW extensional stress regime. Strike slip deformation is very minor, apart from the accommodation zones that segmented this part of the rift.

GEOLOGICAL AND TECTONIC SETTING

The study area is located within the SMO, which constitutes the largest silicic igneous province in North America and the most recent event of this kind on Earth (Ferrari *et al.*, 2007, Bryan and Ferrari, 2013). A distinctive trait of the SMO is the thick late Eocene to early Miocene ignimbrite cover that caps most of the province, traditionally known as the Upper Volcanic Supergroup (UVS, McDowell and Keizer, 1977). The UVS overlies the so-called Lower Volcanic Complex (LVC), constituted by a series of Late Cretaceous to early Eocene batholitic rocks and intermediate lavas, partly coeval with the Peninsular Range Batholiths of Baja California (McDowell and Clabaugh, 1979; McDowell *et al.*, 1997).

The UVS was emplaced approximately between 38 and 18 Ma, with a minimum estimated volume of ~400,000 km^3 of dominantly rhyolitic ignimbrites (~85%) and lesser rhyolitic domes and basaltic lavas. Geochronologic studies have revealed that ignimbrites were erupted in short time spans, with peaks of over 1 km thick ignimbrite sequences emplaced in less than 1 m.y. (Swanson *et al.*, 2006; Ferrari *et al.*, 2002, 2007), implying a high rate of magma generation and eruption (Bryan *et al.*, 2008; Bryan and Ferrari, 2013). Two main flare-up episodes are recognized at ~34–28 Ma and ~24–18 Ma (Ferrari *et al.*, 2007). The Oligocene episode (~34–28 Ma) forms three-quarters of the total erupted volume, covering ~400,000 km^2 of the SMO (Figure 1). The Miocene ignimbritic pulse (~24–18 Ma) is concentrated in the southwestern and western part of the SMO and Baja California (Figure 1) (Sawlan and Smith, 1984; Umhoefer *et al.*, 2001; Drake, 2005; Ferrari *et al.*, 2002, 2007). During this period, volcanism was bimodal, with massive rhyolitic ignimbrites and rhyolitic domes accompanied by basaltic lavas that erupted from fissures, concurrently with extensional faulting (Ferrari *et al.*, 2013). Recent studies in the southern Gulf of California documented the occurrence of early Miocene granitoids and ignimbrites on continental blocks that make up the submerged rifted margins of the Gulf of California rift, suggesting that the source area of the Miocene ignimbrites was located not only in the western side of the SMO but also within the proto-Gulf area (Ferrari *et al.*, 2013; Duque-Trujillo *et al.*, in press).

The central part of the SMO in western Durango and southwestern Chihuahua is characterized by a plateau of flat lying ignimbrites, which appear unfaulted (Henry and Aranda-Gómez. 2000; Ferrari *et al.*, 2007). On both flanks of this unextended core, extensional fault systems tilted the ignimbrite succession in different directions. Geophysical studies indicate a crustal thickness of 40 to 55 km in the unextended core of the SMO (Couch *et al.*, 1991; Bonner and Herrin, 1999), which decreases to ~22–26 km on the extended western flank, adjacent to the Gulf of California (Persaud *et al.*, 2007; Lizarralde *et al.*, 2007; Savage and Wang, 2012) (Figure 1). The extensional fault systems along the western flank of the SMO, in Sonora, Sinaloa, and northern Nayarit are part of the so-called Gulf Extensional Province (GEP), whose onset has been now dated as early as late Oligocene (Murray *et al.*, 2013; Ferrari *et al.*, 2013). Along this belt, ignimbrites are tilted to the ENE or WSW in domains separated by ~ENE-WSW accommodation zones (Stewart, 1998; Ferrari *et al.*, 2007, 2013). Based on the dominant dip direction, tectonic transport direction during rifting, and the type of basement, Ferrari *et al.* (2013) divided the southern SMO into three different domains bounded by accommodation zones where the structural style changes and dip polarity reverses. The studied area is located in the northern Nayarit domain

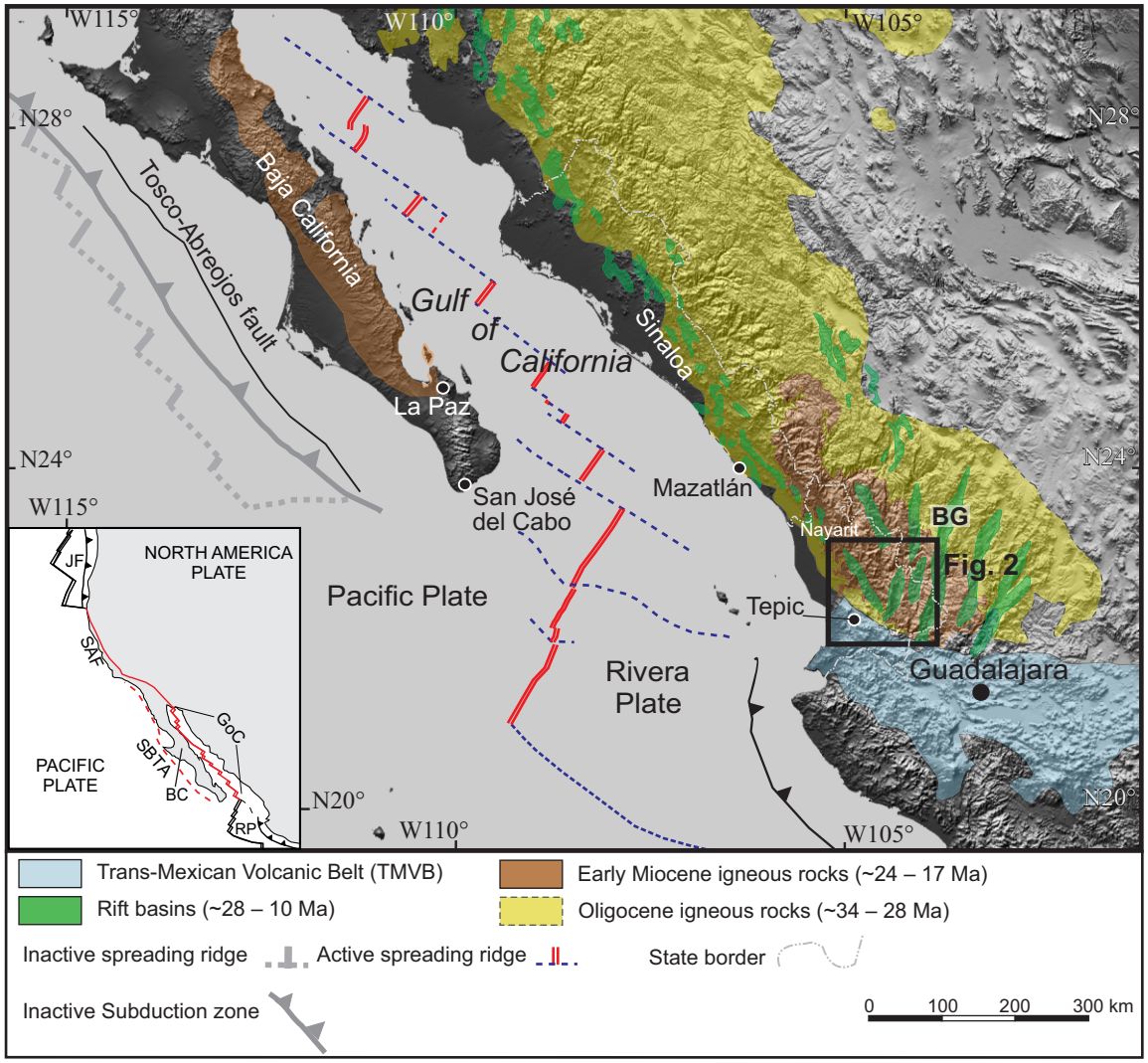

Figure 1. Geodynamic map of western Mexico showing the distribution of the main volcanic provinces and the main regional tectonic features. BG = Bolaños graben. Modified from Duque *et al.* (in press), Bryan and Ferrari (2013), and Ferrari *et al.* (2002). Insert shows the regional geodynamic setting of the Gulf of California. BC: Baja California; SBTA: San Benito-Tosco Abreojos fault system; GoC: Gulf of California; RP: Rivera Plate; JF: Juan de Fuca plate; SAF: San Andreas Fault.

as defined in Ferrari *et al.* (2013), which is bounded to the south by El Roble accommodation zone (Figure 2), a left-lateral shear zone, and to the north, by the Mezquital accommodation zone, which separates opposite tilting of strata (ENE to the south and WSW to the north). Within the northern Nayarit domain, ignimbrites dominantly dip E to ENE due to N-S to NNW-SSE striking west dipping normal faults (Figure 2). Deformation within the northern Nayarit domain can be further separated into eastern and western zones.

The eastern part of the northern Nayarit domain is characterized by N-S striking high-angle normal faults that affect almost the entire domain, forming several graben and half graben structures(Figure 1). This deformation, bracketed between *ca.* 24 and 18 Ma, took place during the first phase of rifting that affected a wide region of the SMO (Ferrari *et al.*, 2013). The western limit of this early extension is difficult to establish because of younger faulting affecting the southeastern margin of the Gulf of California and because structures are probably buried in the coastal plain and offshore in the continental platform. Nevertheless, early Miocene plutons, exposed along the Nayarit coast, on islands just offshore of southeastern Baja California, and on the rifted blocks submerged under the Gulf of California waters, indicate rapid cooling before ~18 Ma, during a major phase of crustal thinning (Duque-Trujillo *et al.*, in press).

The western deformation zone of the northern Nayarit domain is characterized by a 20 km wide and ~160 km long NNW striking belt of extensional fault systems developed along the western margin of the SMO (Pochotitán and San Pedro-Acaponeta fault systems, Figure 2), which accommodated up to ~1.7 km of vertical displacement. These fault systems tilt the 21 to 18 Ma old ignimbrites and rhyolitic lavas up to 35° down to the ENE. The observed field relationships and available ages, indicate that the activity of these fault systems began after ~21 Ma, and they possibly acted as conduits for easy ascent to the surface of small volumes of silicic magmas that extruded as domes or formed subvolcanic intrusions dated between 20 and 17 Ma (Ferrari *et al.*, 2002, 2013). The upper age of these faults is constrained by several 11 to 10 Ma old flat-lying basaltic lavas emplaced along the Nayarit coast that unconformably overlie the SMO ignimbrites. Vertical to very gently dipping, NNW striking mafic dikes of the same age are also intruded parallel to the Pochotitán and San Pedro-Acaponeta fault systems (Righter *et al.*, 1995; Henry and Aranda-Gómez, 2000; Ferrari *et al.*, 2000a, 2002, 2013).

LOCAL GEOLOGY

We closely examined the fault systems along the western flank of the southern SMO, following three transects, which cross the main structures along roads that were recently enlarged and paved, so that fault planes are well exposed along roadcuts (Figure 2 and 3a–3m). A brief description of the geology along these transects (Figures 4 to 6) is given in the following. Geological cross sections (Figure 7) were drawn using information gathered during fieldwork, Google Earth observations, and information compiled from previous works (Ferrari *et al.*, 2002, 2013; SGM, 1998 and 1999).

Northern transect: Estación Ruiz – Jesús María

The Estación Ruiz-Jesús María transect runs approximately in a WSW-ENE direction between the coastal plain and the core of the SMO (Figure 2). It crosses the San Pedro-Acaponeta fault system and the southern part of the Nayar caldera, ending in the Jesús María half graben (Figures 2, 4 and 7a), The oldest rocks of the SMO province are exposed in the lowest part of the sequence on both western and eastern sides of the transect (Figure 7a). These are composed of reddish sandstones and conglomerates (Emvs) rich in andesitic clasts, conglomeratic sandstones, and sandstones interbedded with andesitic lava flows and some thin ignimbrites (Emig) (Figure 3a-3b). Based on crude layering, it can be inferred that this sequence dips ~20° to the east, both on the western and eastern sides of the transect. These deposits are usually too weathered to be dated and are inferred to be of Paleocene to Eocene age in the Mexican Geological Survey geologic maps (SGM, 1996, 1998, 1999, 2006). However, a sample from a 2 m thick ignimbrite (Emig) interbedded with red sandstones (Emvs) along this transect (Figure 3b) has been recently dated at 23.6±0.2 Ma (Ferrari *et al.*, 2013). This age correspond to the onset of the early Miocene ignimbrite pulse in the southern SMO (Scheubel *et al.*, 1988; Ferrari *et al.*, 2002, 2007, 2013; McDowell and McIntosh, 2012). Particularly, ignimbrites of this age make up the Las Canoas ignimbrite succession (Ferrari *et al.*, 2002) exposed in the eastern part of the transect, which covers the reddish volcano-sedimentary sequence. Las Canoas succession is composed of a series of pink to grey, moderately indurated and slightly weathered ignimbrites (Emig), that contain small phenocrysts of plagioclase, biotite, alkali-feldspar and scarce hornblende (Figure 3c). Therefore, the volcaniclastic succession observed in the western part of the transect represents distal facies of the early Miocene volcanic succession exposed in the SMO core (Figure 7a).

A series of mafic dikes (Md), which vary in thickness and orientation, is observed at several locations along the transect cutting the Las Canoas ignimbrites and the volcaniclastic succession. The dikes are dark green, aphyric to porphyritic in texture, with plagioclase and less common hornblende phenocrysts. Most of them have been intruded along fault planes (Figure 3d). Striae and fault gouge (Fg) were observed along some dike walls, indicating that faults remained active after dike intrusion (Figure 3d). In some cases, dikes were cut and displaced by faults (Figure 3e). Intense alteration prevented radiometric dating on most of these mafic dikes. Nevertheless, we were able to obtain a ^{40}Ar-^{39}Ar age for one dike located ~6 km west of Jesús María (site Nay-21, Figure 4). This dike has an E-W orientation and cut an ignimbrite succession that can be correlated with the Las Canoas ignimbrite succession. Two laser step-heating experiments on groundmass concentrates (Figure 8a) yielded similar age spectra, with a decreasing staircase pattern. A plateau age of 23.44±0.23 Ma is defined by five consecutive fractions representing more than 70% of the ^{39}Ar released. The staircase shaped age spectrum suggest the presence of excess argon, for this reason the preferred age was obtained combining all gas fractions obtained from both experiments on a correlation diagram (Figure 8b), which yields a 23.01±0.24 Ma isochron age. A summary of relevant information about ^{40}Ar-^{39}Ar dating is presented in Supplemental file 1. East of Jesús María, a N-S trending mafic dike was also observed cutting the Las Canoas ignimbrite succession and feeding a lava flow (Figure 3c). This dike was too altered to be dated but similar basaltic lavas were dated by Ferrari *et al.* (2002) at 21.3±0.3 Ma just 1.5 km East from this site (their sample TS-21). Based on these two ages and crosscutting relations, we consider that the mafic dikes observed along the eastern part of the transect are early Miocene in age. Basaltic dikes and flows of this age have been also reported for the Bolaños graben (Figure 1) (Nieto-Obregon *et al.*, 1981; Scheubel *et al.*, 1988; Ramos Rosique, 2013) and at the boundary between the SMO and the Trans-Mexican Volcanic Belt north of Guadalajara (Rossotti *et al.*, 2002).

In the central part of the transect, the Las Canoas ignimbrite succession is overlain by the younger Nayar ignimbrite (Nig) succession (Figure 7a) (Ferrari, *et al.*, 2002), which consists of a series of welded ash-flow and air fall tuffs, characterized by white to light yellow colors, composed of ash with phenocrysts of quartz, plagioclase, alkali-feldspar and biotite (Figure 3f). Several rhyolitic domes (Rd) are intercalated with or cap the Nayarit ignimbritic succession (Figure 3g to 3i; Figure 7a). These domes, which post-date the Nayar succession, yielded ages between ~17.5 and 18.4 Ma (Figure 4) (Ferrari *et al.*, 2002; 2013). In the Mesa del Nayar area most layers of this succession are horizontal or show only minor tilting (<10°), whereas they are tilted up to 35° to the west (Figures 2 and 3f). The maximum thickness of the Nayar succession is observed in the Mesa del Nayar area (Figure 3i), with at least ~800 m of ignimbrites (Figure 7a). The top and the base of the unit were dated by Ferrari *et al.* (2002) at 19.9±0.4 Ma and 21.1±0.3 Ma, respectively, implying that a thickness of almost 1 km was emplaced within *ca.* 1 m.y. The source of this succession has been associated with the formation of a series of NNW aligned calderas, interpreted on the basis of landforms, domes, and sedimentary deposits found in the Mesa del Nayar area (Ferrari *et al.*, 2002).

Central transect: Aguamilpa dam

This relatively short transect runs for ~12 km in a WSW-ENE direction along roads following both sides of the Santiago river, downstream and west of the Aguamilpa dam (Figures 2 and 5). In this area, the Santiago river follows a complex accommodation zone, which separates the San Pedro-Acaponeta fault system to the north from the Pochotitán fault system to the south (Figure 2). The geology of the Aguamilpa dam area is dominated by a succession of well indurated, pink colored ignimbrites, typically rich in phenocrysts of plagioclase and/or biotite. The succession dips 26° to 50° to the W and WSW due to normal faulting (Figure 7b). Available ages for these ignimbrites range between 22.4 and 18.7 Ma (Rodríguez-Castañeda and Rodríguez-Torres, 1992, and references therein; Frey *et al.*, 2007), making them broadly correlative with the Las Canoas and the Nayar successions.

A series of subvolcanic bodies, which vary in composition from intermediate to felsic, are found below the ignimbrites (Figure 7b). Although field relations are not always clear, some of them are clearly intrusive and seem to have exploited the normal faults to ascend to a shallow level. Rodríguez-Castañeda and Rodríguez-Torres (1992) report a K-Ar age of 18.3 Ma for an granite body. Duque-Trujillo *et al.* (in press) report many subvolcanic intrusives along the SMO piedmont with ages between 22.3 and 18.1 Ma. Based on their geographical distribution, mineralogy, and field relationship with the ignimbrites, we consider that the subvolcanic bodies exposed near the Aguamilpa dam are part of the same subvolcanic suite.

Several rhyolitic domes cap the ignimbrites (Figures 2, 5 and 7b). Although no dates have been obtained, their stratigraphic position

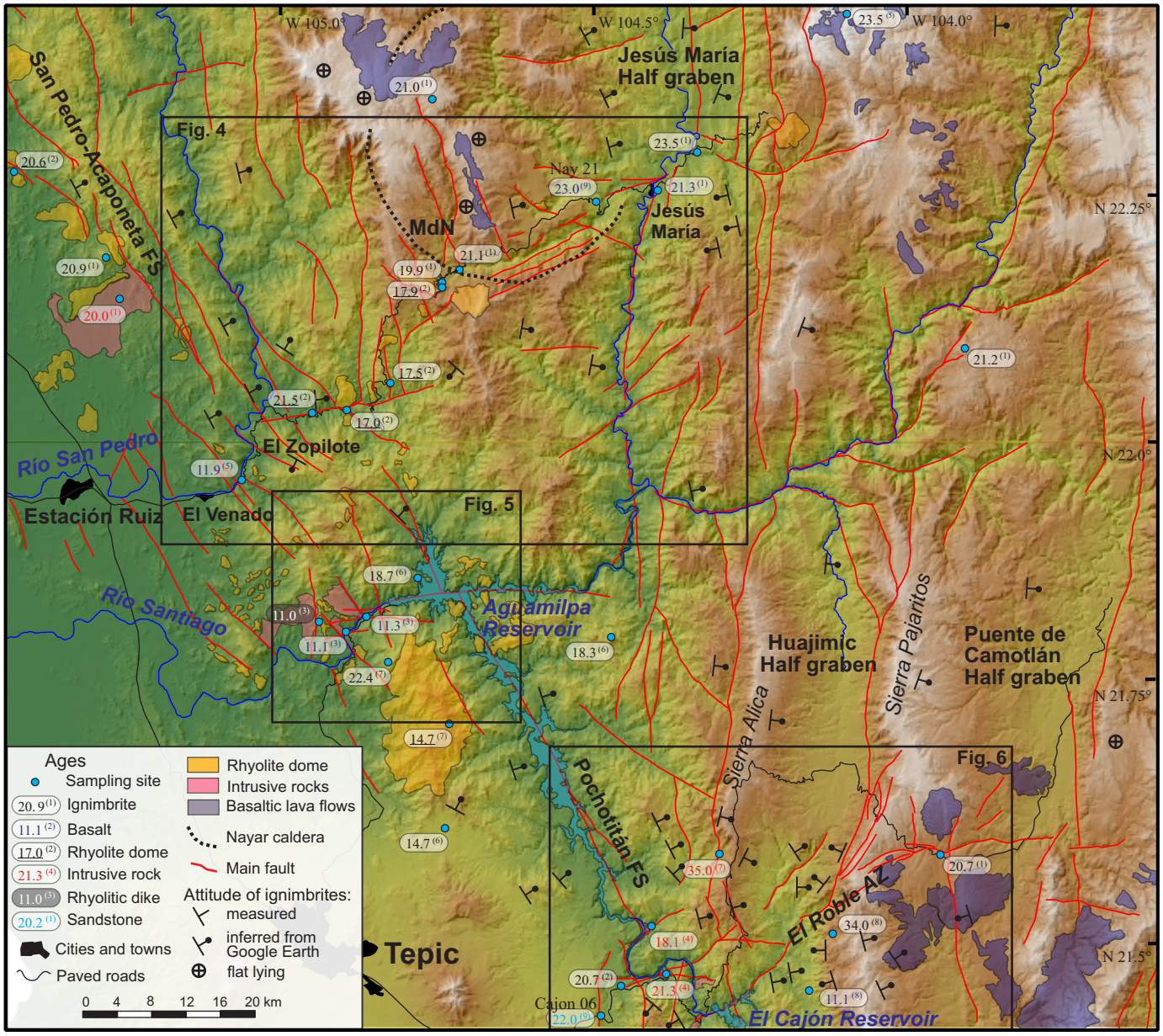

Figure 2. Map of the study area showing selected geological features and isotopic ages described in the text. Minor faults interpreted during the present work; main fault traces from Ferrari *et al.* (2013). Dip directions from Ferrari *et al.* (2002, 2013), 1:250.000 scale geologic maps of Servicio Geológico Méxicano (Escuinapa and Tepic sheets), and Google Earth observations. Reference for geochronologic dates, shown in parentheses on each date: (1) Ferrari *et al.* (2002); (2) Ferrari *et al.* (2013); (3) Frey *et al.* (2007); (4) Duque-Trujillo *et al.* (in press); (5) Clark *et al.* (1981); (6) Soto and Ortega (1982); (7) Rodríguez-Castañeda and Rodríguez-Torres (1992); (8) Damon *et al.*, 1979; (9) This study. FS: Fault system, AZ: Accommodation zone.

suggests that they could correlate with those observed in the Estación Ruiz-Jesús María transect east of Mesa del Nayar, with ages between ~17.5 and 18.4 Ma. A large dome complex is also observed on the southwestern side of the Aguamilpa reservoir. Rodríguez-Castañeda and Rodríguez-Torres (1992) report a K-Ar age of 14.7 Ma for an andesite making up the peak of the complex (Picachos andesite). Although these domes were not mapped in detail, they do not appear faulted, suggesting they post-date the NNW striking normal fault systems.

A swarm of mafic dikes cross-cut the early Miocene ignimbrites along this transect. They are fine grained to aphyric, dark green in color and range between 1 to 4 m in thickness. Many of these dikes were dated both by K-Ar and ^{40}Ar-^{39}Ar methods, yielding ages between 11.5 and 11 Ma (Damon *et al.*, 1979; Soto and Ortega, 1982; Frey *et al.*, 2007). These dikes are thus part of the regional pulse of mafic magmatism recognized along the whole eastern side of the Gulf, as described and discussed in Ferrari *et al.* (2013).

Southern transect: El Cajón – Sierra de Pajaritos

This transect goes from Santa María del Oro-El Cajón area, at the boundary between the Trans Mexican Volcanic Belt (TMVB) and the SMO (Figure 7c), to the Sierra de Pajaritos fault system, which bounds the eastern side of the Huajimic half graben (Figures 2 and 7d). This transect passes across the NNW striking Pochotitán fault system and the N-S striking Sierra de Alica fault system and, in its

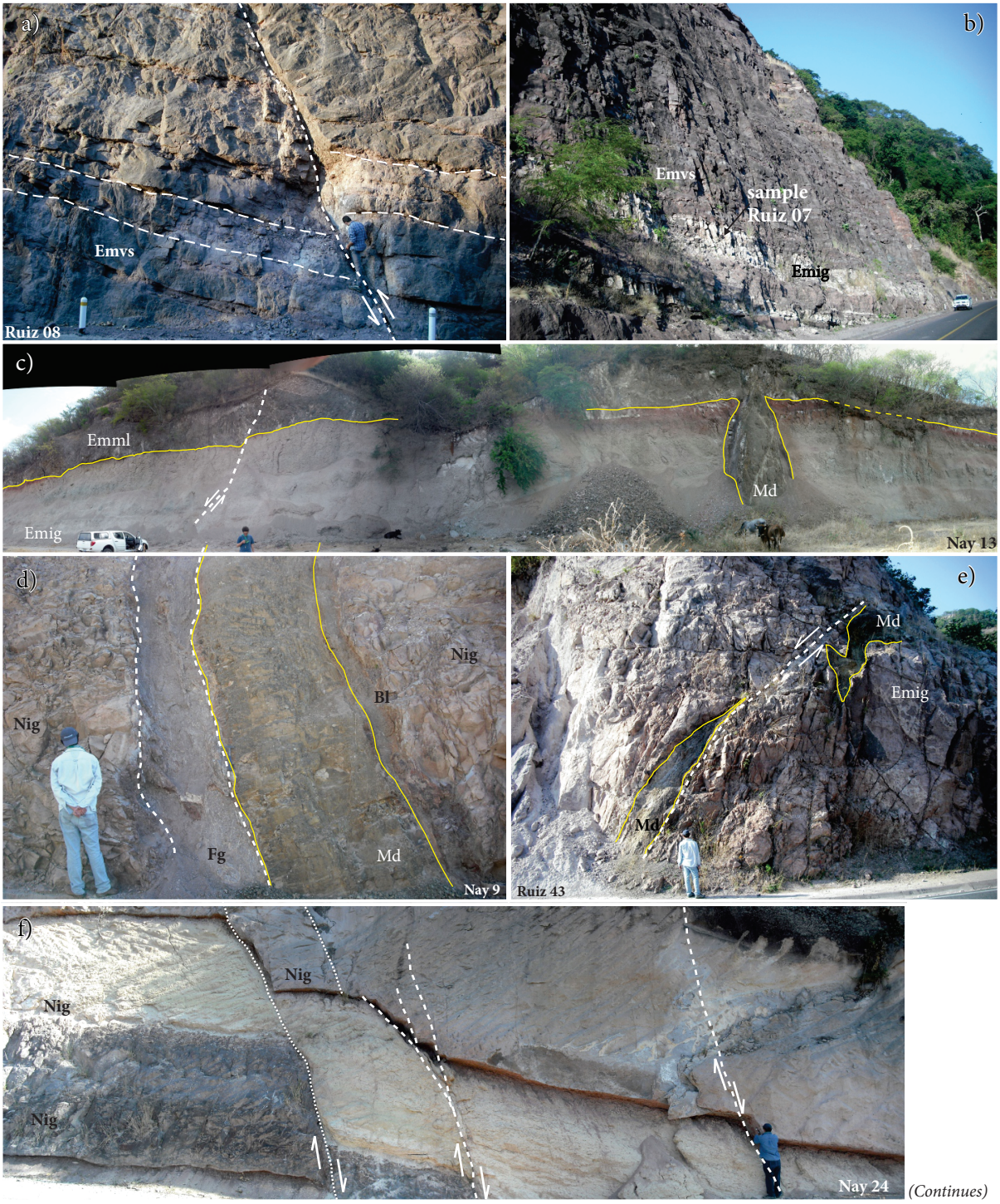

(Continues)

Figure 3. a) NE-verging oblique reverse fault affecting volcanoclastic deposits (Emvs) at the base of the El Nayar ignimbrite succession; site Ruiz-08. Picture taken at 22.0345°N, 104.9063°W, looking north. b) Ignimbrite (Emig), dated at 23.6±0.2 Ma (sample Ruiz 07; Ferrari *et al.*, 2013), interbedded with a volcanoclastic deposit (Emvs). Picture taken at 22.0295°N, 104.8869°W, looking north. c) A mafic dike (Md) cutting an ignimbrite (Emig) correlative with the Canoas succession and feeding a basaltic lava flow (Emml), cut by a small E-dipping normal fault; site Nay-13. Picture taken at 22.2515°N, 104.5263°W, looking southeast. d) Fault gouge at the contact between a mafic dike (Md) and the El Nayar ignimbrites (Nig) at site Nay-09. Picture taken at 22.1893°N, 104.6782°W, looking south. Fg: Fault gauge; Bl: baked layer. e) Mafic dike (Md) intruding early Miocene ignimbrite (Emig) and displaced by a W-dipping normal fault at site Ruiz-43. Picture taken at 22.0377° N, 104.8406°W, looking northwest. f) A series of SW-dipping normal faults cutting the El Nayar ignimbrites (Nig) at site Nay-24. Picture taken at 22.2316°N, 104.6174°W, looking east. (*continues*)

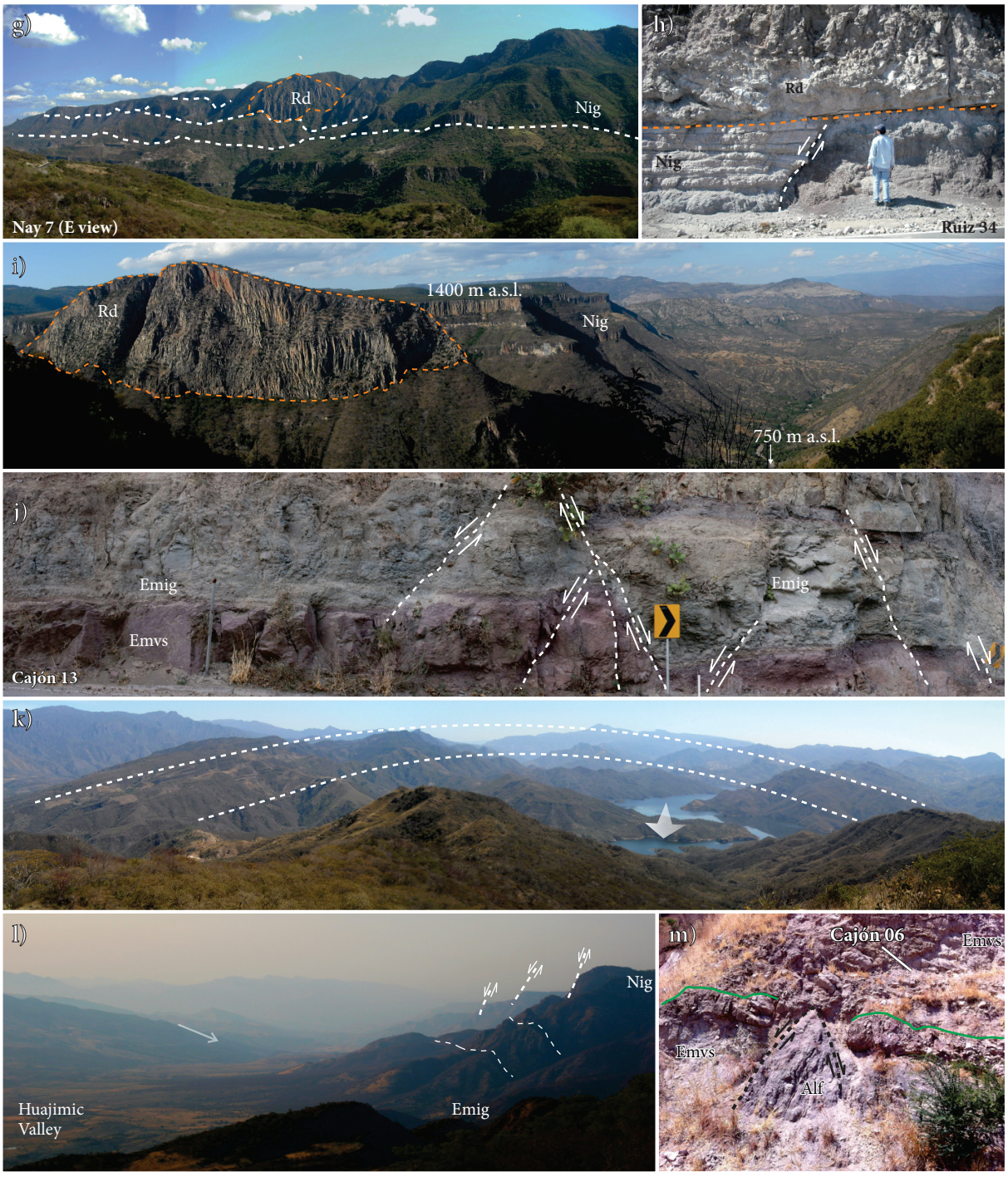

Figure 3 (cont.). g) Traces (white doted lines) of N-dipping normal faults affecting the upper part of the El Nayar succession (Nig). Picture taken at 22.18702°N, 104.69260°W, looking east. h) E-dipping normal fault covered by a rhyolitic dome (Rd) dated at 17.57±0.19 Ma by ^{40}Ar-^{39}Ar in biotite (Ferrari *et al.* 2013), site Ruiz-34. Picture taken at 22.18702°N, 104.69260°W, looking east. i) The ~800 m thick El Nayar ignimbritic sequence (Nig), capped by a rhyolitic dome (Rd) at Mesa del Nayar. Picture taken at 22.2189°N, 104.6412°W, looking northeast. m a.s.l.: meters above sea level. j) Eocene volcano-sedimentary sequence (Emvs) underlying early Miocene ignimbrite and affected by conjugate normal faulting near Santiago river, site Cajón 13. Picture taken at 22.4381°N, 104.4876°W, looking east. k) Broad anticline formed by the Miocene ignimbrites in the El Cajón reservoir zone. Picture taken at 21.4541°N, 104.4454°W, looking southwest. Fold axis and plunging north (white arrow). l) Trace and vertical projection of some west-dipping normal faults on the Sierra de Pajaritos escarpment. On the west side of the Huajimic valley, the El Nayar ignimbrite sequences (Nig) dip to the east (arrow). Picture taken at 21.6268°N, 104.2698°W, looking north. m) Normal fault affecting an andesitic lava flow (Alf) and covered by a reddish volcano-sedimetary deposit (Emvs; sample Cajón 06). La línea verde marca el límite entre la secuencia afectada por el fallamiento y la no afectada. Picture taken at 22.4278°N, 104.5761°W, looking east.

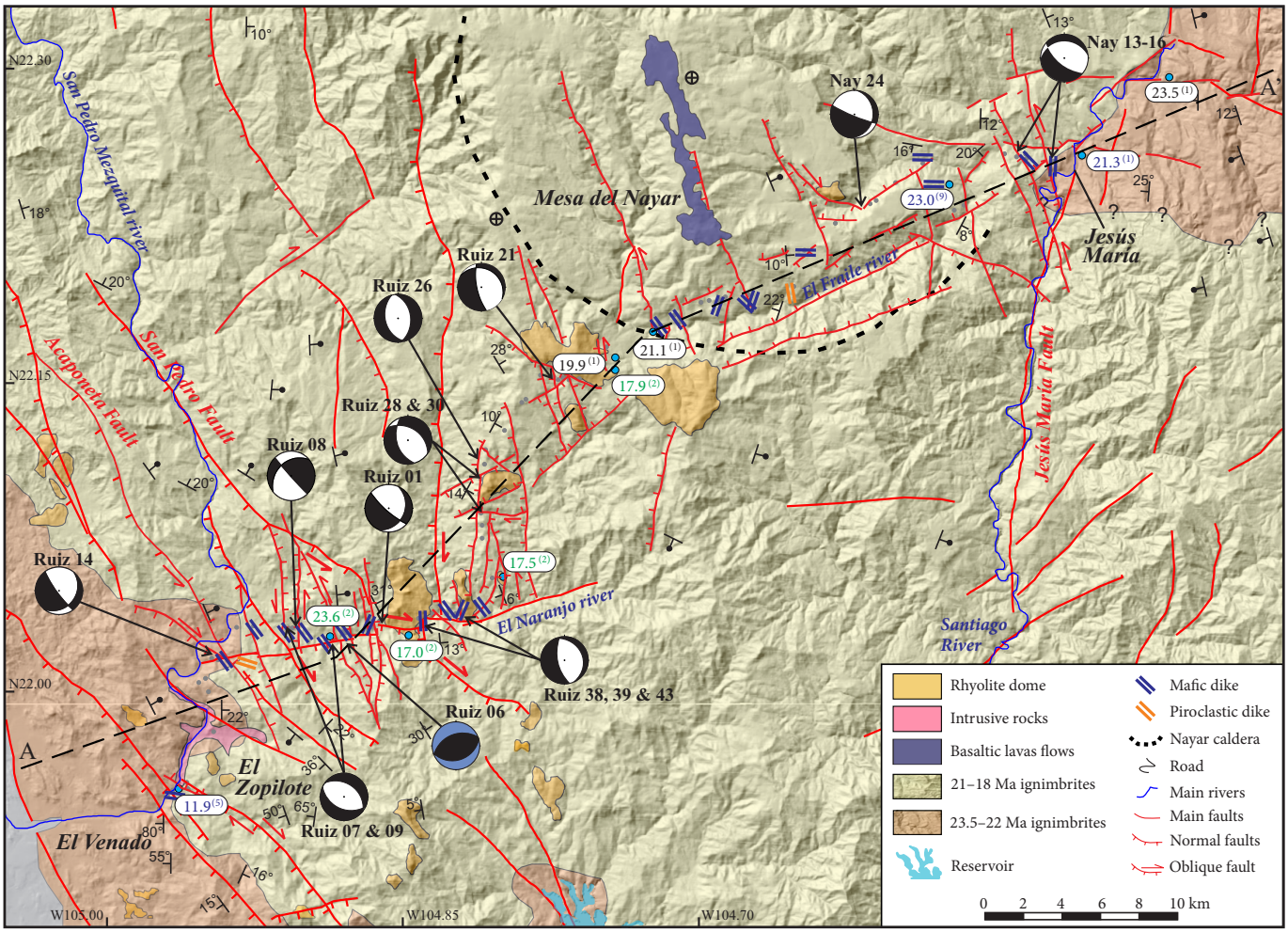

Figure 4. Geological map of the Estación Ruiz – Jesús María transect showing fault kinematics and right-dihedra solution obtained from field data. On the right-dihedra diagrams, black quadrants indicate tension and white quadrants indicate compression. The Ruiz 06 dihedra diagram (blue compressive quadrants) represents a local situation (see text for explanation). Minor faults interpreted in this work, and main fault traces from Ferrari *et al.* (2013). Dip directions from Ferrari *et al.* (2002, 2013), 1:250.000 scale geologic maps of Servicio Geológico Méxicano, Escuinapa and Tepic sheets, (SGM, 1998, 1999), and Google Earth observations. Key for ages as in Figure 2.

eastern part, intersects the Sierra de Pajaritos fault system and El Roble accommodation zone (Figures 6 and 7c-7d). The geologic units observed along this transect are similar to those described in the other two transects.

The lower part of the sequence observed along this transect is constituted by a reddish volcano-sedimentary sequence (Emvs), mainly composed of sandstones and conglomeratic sandstones with abundant clasts of andesitic volcanic rocks (Figures 3j and 7c). Interbedded within this sequence are ignimbrites (Emig) that range in thickness from 2 to >50 m, which become dominant up-section. Ignimbrites vary in composition; they are characterized by different matrix color, phenocrysts, fiammes and lithics of different compositions. Also, interbedded in the volcano-sedimentary sequence are andesitic lava flows, usually less than 5 m thick. These are fine to medium grained, usually porphyritic with hornblende and plagioclase phenocrysts. On the western side of the El Cajón reservoir, the dip of this sequence varies greatly, but does not exceed 30°; strata mainly dips west with variation from WSW to NNW. On the eastern side of the El Cajón reservoir, rocks dips mostly to the east, defining a broad anticline with a N-S striking axial plane parallel to the valley (Figures 3k and 7c). This is part of a series of left-stepping en-echelon folds developed by left-lateral transpression along the boundary between the SMO and the TMVB, which would have been active between 14.5 and 11.5 Ma (Ferrari, 1995; Ferrari *et al.*, 2002). North of the transect, at Sierra de Alica and Sierra de Pajaritos, rocks dip monotonously to the east because of N-S striking west-dipping normal faults (Figures 2, 3l and 7d).

Despite the lack of radiometric ages, in the geologic maps of the Mexican Geological Survey (SGM, 1996, 1998), the lower part of the succession in this area is interpreted as Paleocene to Oligocene in age. Middle and late Eocene ages have been reported for a rhyolite lava and an ignimbrite northwest of Santa María del Oro and southern Sierra de Pajaritos, respectively (Damon, *et al.*, 1979; Frey *et al.*, 2007), but the geologic context of these samples is unknown. We dated detrital zircons separated from the sandy matrix of the reddish volcano-sedimentary succession toward the base of the succession (sample Cajón 06, Figure 9). The dated layer include well rounded green and red clasts of porphyritic volcanic rocks and overlies a faulted sequence of red sandstones and siltstones (Emvs), in turn deposited over a basaltic lava flow (Figures 3m and 8). Twenty-seven grains yielded ages in the range between 26 and 22 Ma, with a peak at ~23.5 Ma, indicating that this sequence is correlative with that found in the lower part of the Estación Ruiz-Jesús María transect.

The upper part of the sequence is dominated by several ignimbrites that resemble the Nayar succession (Figure 7c). These are white to light yellow ash flow tuffs, with phenocrysts of plagioclase, K-feldspar, quartz and biotite in a matrix composed mainly of ash and, less commonly, pumice, which may constitute up to 30% of the rock. ^{40}Ar-^{39}Ar ages of 20.5±0.4 Ma and 20.7±0.2 Ma (Ferrari *et al.*, 2002; 2013) confirm that these ignimbrites are distal facies of the Nayar succession.

On the deepest part of the Santiago river, several subvolcanic bodies were found intruding the ignimbrites. Using U-Pb in zircon geochronology, Duque-Trujillo *et al.* (in press) dated a quartz-dioritic and a granitic subvolcanic body from the footwall of the Pochotitán fault system at 18.1±0.2 and 21.3±0.43 Ma, respectively (Figure 6).

A series of mafic dikes cuts the whole volcanic sequence in the El Cajón-Sierra de Pajaritos region. These dikes vary in width and orientation, but have similar appearance, being dark green in color, aphyric to porphyritic, with plagioclase and less often hornblende phenocrysts. Most of them are moderately altered and are surrounded by baked layers of country rock, as in the Estación Ruiz-Jesús María transect (Figure 3d). Dike intrusion mostly occurred along faults, which in some cases were also active after the intrusion, displacing some of the dikes. Damon *et al.* (1979) reported an age of 11.1 Ma for a mafic dike east of El Cajón reservoir. This age, and the fact that the mafic dikes were observed cutting all the early Miocene ignimbrites, indicate that they are coeval with those observed in the Aguamilpa dam area to the north (Figure 5) and with the regional pulse of late Miocene mafic volcanism recognized on the eastern side of the Gulf (Ferrari *et al.*, 2002; 2013).

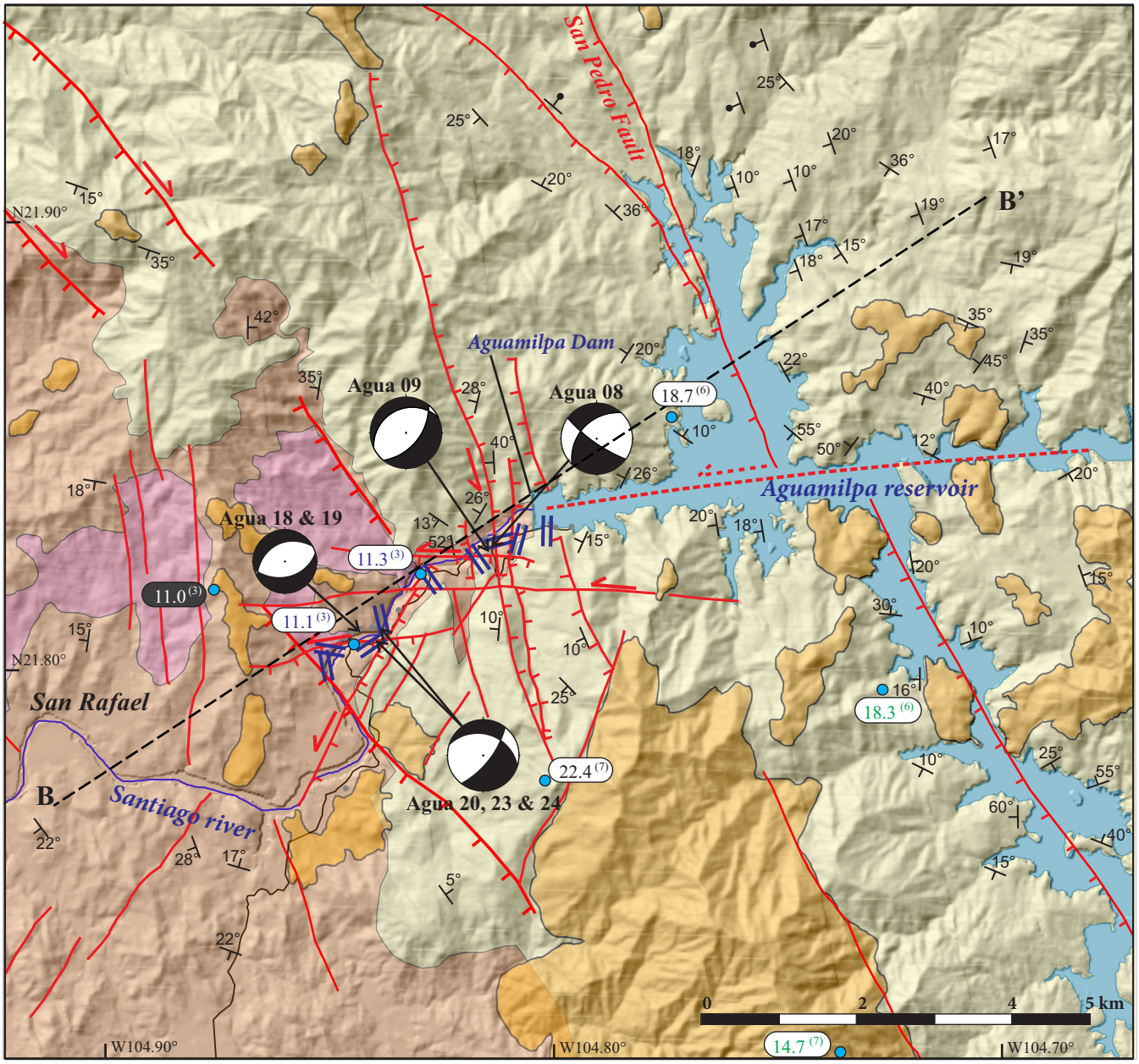

Figure 5. Geological map of the Aguamilpa Dam transect. Minor faults interpreted in this work, and main fault traces from Ferrari *et al.* (2013). On the right-dihedra diagrams, black quadrants indicate tension and white quadrants indicate compression. Dip directions from Ferrari *et al.* (2002, 2013), 1:250.000 scale geologic maps of Servicio Geológico Méxicano, Escuinapa and Tepic sheets, (SGM, 1998; 1999), and Google Earth observations. Key for ages as in Figure 2.

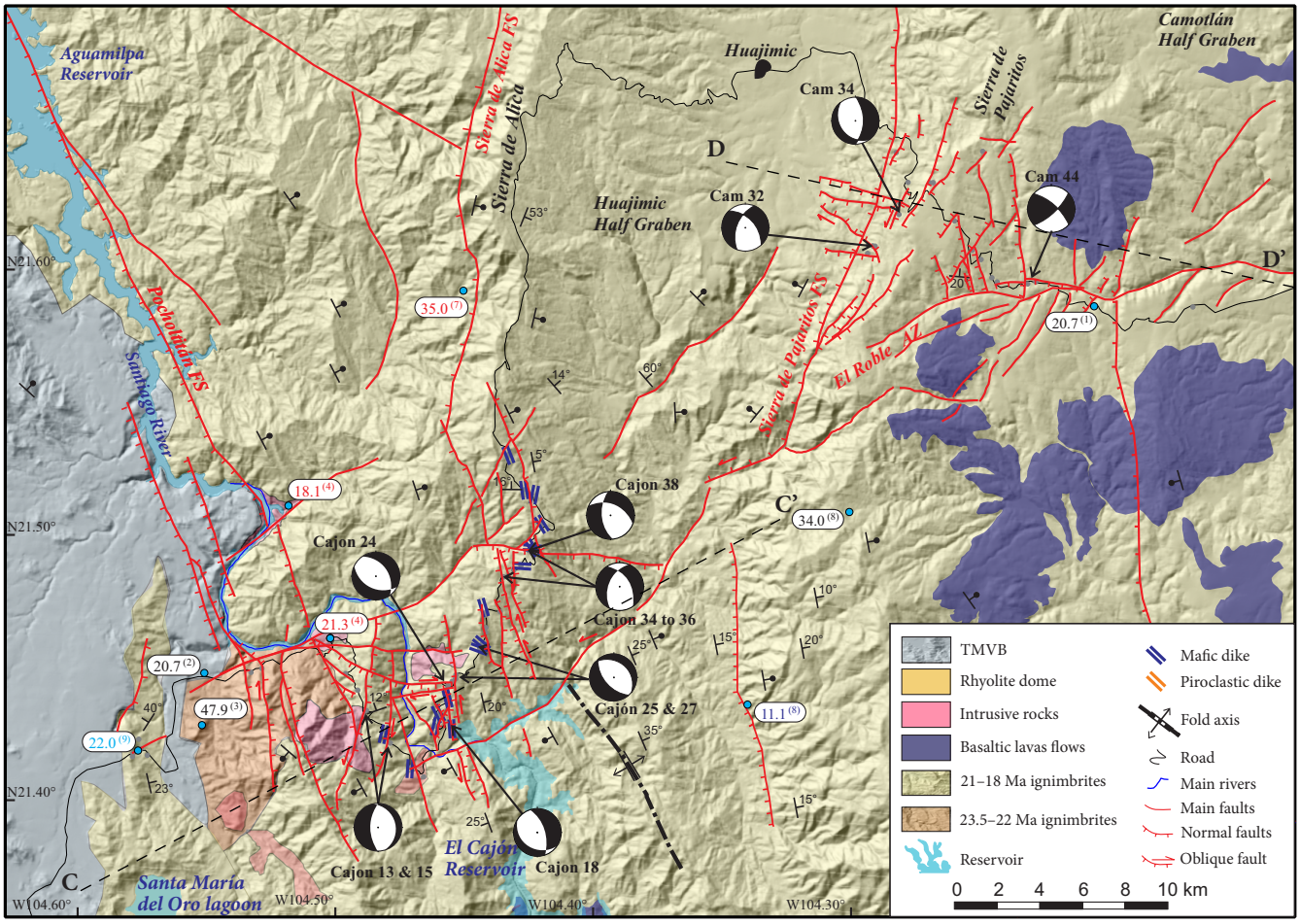

Figure 6. Geological map of the El Cajón – Sierra de Pajaritos transect. On the right-dihedra diagrams, black quadrants indicate tension and white quadrants indicate compression. Dip directions from Ferrari *et al.* (2002, 2013), 1:250.000 scale geologic maps of Servicio Geológico Méxicano, Escuinapa and Tepic sheets, (SGM, 1998; 1999), and Google Earth observations. Key for ages as in Figure 4.

FIELD MEASUREMENTS

A total of 160 faults and 144 dikes were measured along the three transects described in the previous section. Faults and fractures were identified at the outcrop scale, paying particular attention to areas where the roads cross the main fault systems. The orientation of faults and fractures were measured using a stratum compass, and fault planes were inspected for fault-slip kinematic indicators (*e.g.*, slickenlines). Each fault-slip measurement consisted of strike and dip of the fault plane and trend and plunge of the slickenlines. Faults and kinematic indicators were observed at 24 structural outcrops allowing for a dynamic analysis. We performed a paleo-stress analysis using the right-dihedra method of Angelier (1979, 1984) (Table 1; Figures 4-6, and 10) using the tectonicsFP software (Ortner *et al.* 2002). The sum of right-dihedra diagrams defines tension and compression quadrants similar to those used in the visualization of earthquake focal mechanisms. The maximum and minimum stress tensors axis, σ1 and σ3, should be located inside these quadrants (Angelier, 1994). To define the degree of fitting of the data set, right-dihedra density plot from each transect (obtained using the stereo32 software) are shown together with the fault-slip data in Figure 10. The right-dihedra method was applied only at sites where a minimum of four faults with kinematic indicators was observed. However we included three sites (Ruiz 26, Nay 24, and Cam 32) where less than four kinematic indicators were measured because at these sites a major fault plane with homogeneous kinematic indicators was present. All the measured faults and kinematic indicators are contained in the 23.5 Ma and younger volcano-sedimentary sequence, ignimbrites, and mafic dikes. A synthesis of faults, slikenlines, and mafic dikes measurements is presented in Figure 11.

Faults

We summarize the orientations of faults measured along each of the three transects and illustrate the three broad categories of observed fault orientations (Figure 11a–11c). The dominant orientation is N-S to NNW-SSE, which corresponds to the main extensional structures affecting the southern SMO (Ferrari *et al.*, 2007, 2013), and produced up to 100 km long and 20 km wide grabens and half grabens. In the study area, these faults displace the early Miocene ignimbrite succession, forming the Jesús María, Sierra de Alica, and Huajimic half grabens, with offsets up to 1.5 km (Figures 1, 7a, 7c and 7d).

The second dominant fault orientation is NW-SE and corresponds to the San Pedro-Acaponeta and Pochotitán fault systems, located on the westernmost part of the SMO, bordering the coastal plain (Figures 2 and 6). The offset along these faults systems is at least 1 km as they lower the SMO ignimbrites beneath the coastal plain (Figure 7b).

A third group of faults, almost orthogonal to the previous two groups has E-W and NE-SW orientation. These faults correspond to accommodation zones, which separate different segments of the rift

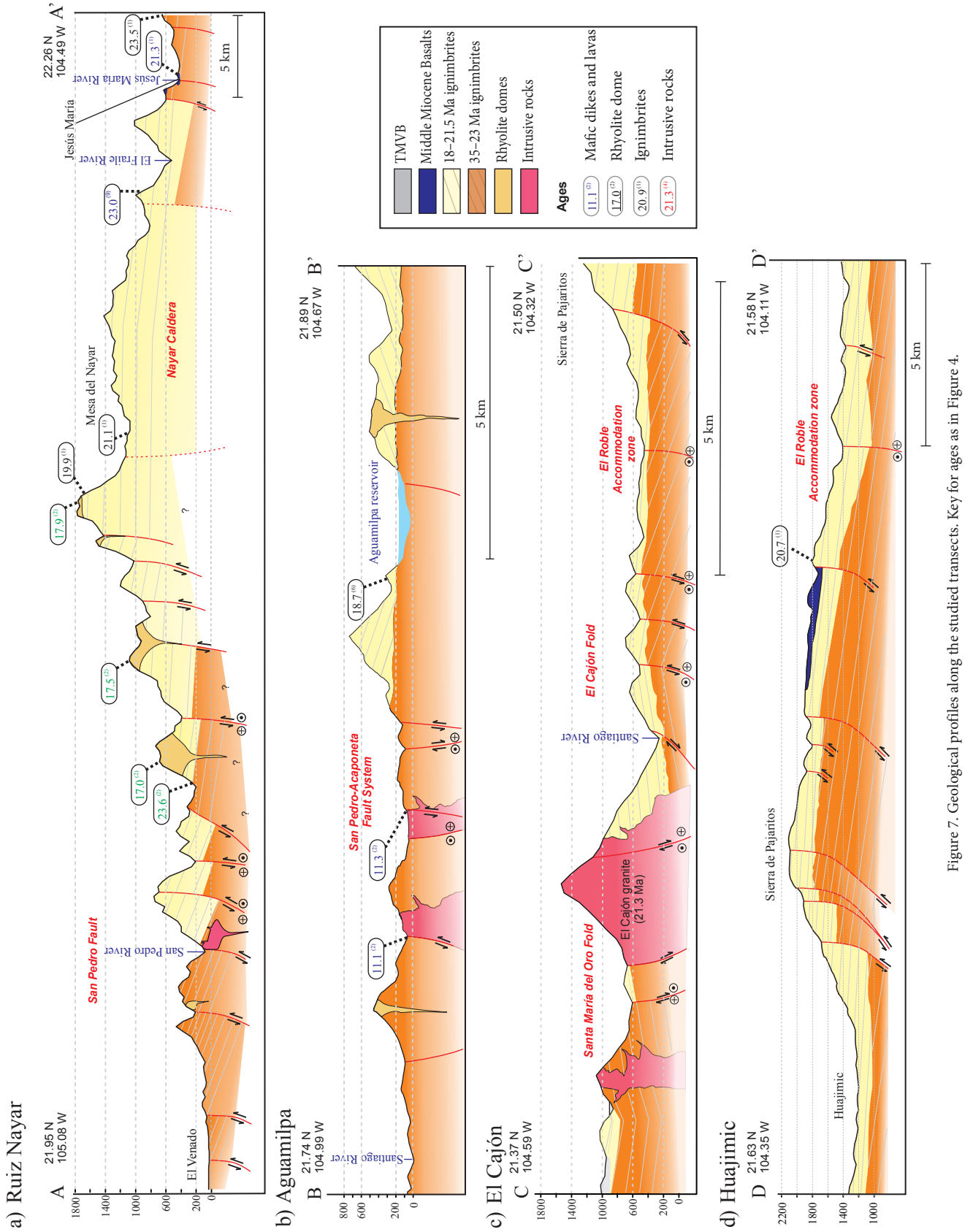

Figure 7. Geological profiles along the studied transects. Key for ages as in Figure 4.

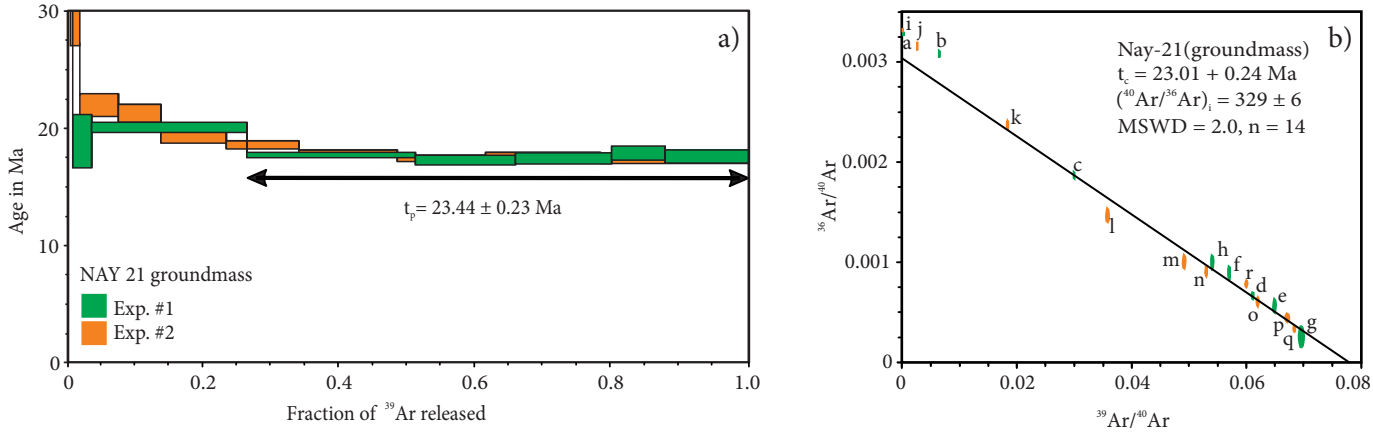

Figure 8. a) ^{40}Ar-^{39}Ar age spectra and b) ^{36}Ar-^{40}Ar versus ^{39}Ar-^{40}Ar correlation diagram for sample Nay 21 (22.24161°N; 104.57821°W). Colors in B represent the two experiments shown in (a). Analytical data are provided in Supplemental file 1.

characterized by opposite tilting direction (Ferrari *et al.*, 2002; 2013). Axen (1995) also observed that the Main Gulf Escarpment in Baja California is segmented by similar accommodation zones.

The field measurements (Figure 11a-11c) show some variation with respect to the large-scale faults and lineations (Figures 4 to 6). This difference is likely due to the presence of several second order structures seen at outcrop scale, such as Riedel shears and tension gashes, which are normally associated with the main structures.

Estación Ruiz-Mesa del Nayar transect

Along this transect, the dominant fault orientation is N-S to NNW-SSE with a dominant dip to the west (Figure 4, Figure 11a). Large blocks of the SMO ignimbrite sequence are tilted ~20° down to the east, with offsets varying from meters to hundreds of meters (Figure 7a). Most faults have normal dip-slip kinematics, but a right-lateral(?) strike-slip component can be observed near the San Pedro-Pochotitán fault system, and is not observed further east (Figure 4). One of the N-S striking faults is capped and sealed by a rhyolitic dome (site Ruiz-34) (Figures 3h and 4) dated at 18.4±0.3 Ma by U-Pb in zircon and 17.57±0.19 Ma by ^{40}Ar-^{39}Ar in biotite (Ferrari *et al.*, 2013). Assuming this single fault is representative of the population of N-S striking faults, this relation implies that the N-S faults where not active after ~18 Ma.

The San Pedro-Pochotitán fault system is present on the westernmost portion of this transect. The faults belonging to this system are characterized by a NW-SE orientation with primarily normal dip-slip kinematics, although a dextral strike-slip component was observed in many of the measured faults. Most of the faults dip to the west, tilting the ignimbrites and sediments of the SMO ~20° down to the east (Figure 7a).

NE-SW and E-W striking faults are also present in this transect. These faults control the El Fraile and El Naranjo rivers (Figure 4). From the western part of Mesa del Nayar to Jesús María, the dominant structures are NE-SW striking faults, NW dipping normal faults located on the southern side of the El Fraile river (Figure 3g), and shorter faults with variable dip on the northern side (Figure 4). The El Fraile river faults have a prominent morphological expression, and Ferrari *et al.* (2002; 2007) interpreted them as part of a caldera rim, with the area to the north of the river forming the caldera interior, filled by numerous ignimbrite sheets (Figure 4). On the western part of the transect, along El Naranjo river, we observed a series of E-W striking and south dipping faults, with a dominant right-lateral strike-slip motion (Figure 4). Some minor reverse faults (blue stereoplot in Figure 4) affecting the volcano-sedimentary and ignimbrite rocks have been interpreted as local restraining segments within the strike-slip system (sites Ruiz-05 and 06 in Figures 3a and 4). The ENE-WSW striking El Fraile fault system and the E-W striking El Naranjo fault system could represent an accommodation zone, likely related to basement discontinuities. At least in some part of the transect, these transverse structures represent a boundary between zones with opposite tilting of the volcano-sedimentary sequence (Figure 2).

Aguamilpa Dam transect

Although the Aguamilpa Dam transect runs along the northern part of the NNW striking Pochotitán fault system, several fault orientations where found. NNE-SSW striking faults are the most abundant structures observed in outcrops (Figure 11b). Most of them are minor faults, with only one major fault showing normal kinematics with a left-lateral strike-slip component of motion (Figure 5). We speculate that these faults could be Riedel structures (R') formed by the activity of the Pochotitán fault system. E-W faults were also observed with dominant normal dip-slip kinematics and a consistent left-lateral component of motion. The E-W faults are arranged in a left stepping array (Figures 2 and 4). Together with the NE-SW faults, they inter-

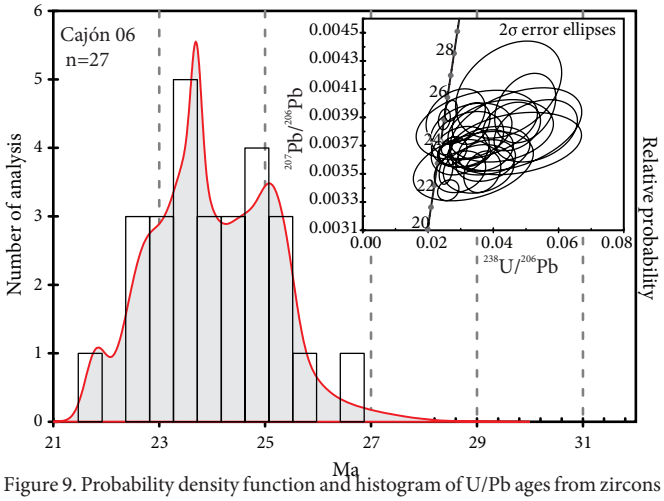

Figure 9. Probability density function and histogram of U/Pb ages from zircons from sample Cajón 06 (21.42845°N; 104.57444°W). Upper right insert shows U/Pb Concordia diagram of analyzed grains. Analytical data are provided in Supplemental file 2.

Table 1. Summary of structural sites, observed lithology and right-dihedra-based paleo-stress tensors (σ1, σ2, and σ3) orientations calculated for each site.

Site	Lat. N	Long. W	Lithology	Lithology age (Ma)	*n*	σ1		σ2		σ3	
Ruiz - Mesa del Nayar Transect						**pl**	**az**	**pl**	**az**	**pl**	**az**
Ruiz 01	22.0378°	-104.8627°	Pink ignimbrite with fiammes	Early Miocene	9	47	009	30	138	28	246
Ruiz 06	22.0326°	-104.8811°	Pink ignimbrite with fiammes	Early Miocene	9	05	340	02	250	85	136
Ruiz 07 and 09	22.0295°	-104.8869°	2 m thick ignimbrites interbedded with redish fluviovolcanic sequence	>21. 5 Ma (1)	4	84	320	06	120	02	211
	22.0344°	-104.9081°									
Ruiz 08	22.0345°	-104.9063°	2 m thick ignimbrites interbedded with redish fluviovolcanic sequence	Early Miocene	9	31	195	40	081	34	081
Ruiz 14	22.0203°	-104.9466°	Andesitic subvolcanic intrusive	Early Miocene	6	46	025	28	148	31	257
Ruiz 21	22.1512°	-104.7755°	White ignimbrite (El Nayar) over fluviovolcanic redish sequence	Early Miocene (18 to 20 Ma)	10	57	099	16	343	28	245
Ruiz 26	22.1174°	-104.8097°	White ignimbrite (El Nayar sequence)	Early Miocene (18 to 20 Ma)	3	86	344	04	169	00	079
Ruiz 28 and 30	22.1037°	-104.8119°	White and pink ignimbrites (El Nayar sequence)	Early Miocene (18 to 20 Ma)	5	68	135	22	325	03	234
	22.0878°	-104.8120°									
Ruiz 38, 39 and 40	22.0399°	-104.8214°	White and pink ignimbrites (El Nayar sequence)	Early Miocene (18 to 20 Ma)	9	69	086	04	346	20	255
	22.0411°	-104.8246°									
Nay 13 to 16	22.2515°	-104.5263°	Brown and pink ignimbrite succession	Oligocene?	6	63	071	18	301	19	204
	22.2534°	-104.5441°									
Nay 24	22.2316°	-104.6174°	Light yellow and pink ignimbrites	Miocene	2	47	359	22	114	35	221
Aguamilpa Transect											
Agua 08	21.8314°	-104.8082°	Light pink ignimbrite	Early Miocene	8	35	077	49	294	19	180
Agua 09	21.8331°	-104.8120°	Light pink ignimbrite	Early Miocene	9	72	276	12	046	13	139
Agua 18 and 19	21.8249°	-104.8439°	Gray lithic ignimbrite	Early Miocene	4	87	104	03	267	01	357
	21.8132°	-104.8412°									
Agua 20, 23 and 24	21.8135°	-104.8396°	Gray lithic ignimbrite	Early Miocene	5	48	268	35	50	20	155
	21.8106°	-104.8404°									
El Cajón-Sierra de Pajaritos Transect											
Cajón 13 and 15	21.4381°	-104.4876°	Fluvio-volcanic sequence with interbedded ignimbrites	Early Miocene	6	70	105	06	358	19	266
	21.4264°	-104.4783°									
Cajón 18	21.4326°	-104.4545°	Well indurated lithic ignimbrite	Early Miocene	9	65	286	17	153	17	058
Cajón 24	21.4487°	-104.4543°	Fluvio-volcanic sequence	Early Miocene	15	74	310	16	131	00	041
Cajón 25 and 27	21.4496°	-104.4530°	Pink ignimbrites over basaltic andesite lava flow	Early Miocene	9	79	64	3	317	11	227
	21.4606°	-104.4436°									
Cajón 34 to 36	21.4865°	-104.4343°	White crystal rich ignimbrite	Early Miocene	7	56	182	34	358	03	088
	21.4889°	-104.4304°									
Cajón 38	21.4960°	-104.4246°	White crystal rich ignimbrite	Early Miocene	4	54	139	36	329	05	238
Cam 32	21.6061°	-104.2899°	White to pale yellow ignimbrite	Early Miocene	1	50	168	40	350	01	259
Cam 34	21.6175°	-104.2807°	White to pale yellow ignimbrite	Early Miocene	9	65	307	18	172	16	076
Cam 44	21.5924°	-104.2306°	Pink well indurated ignimbrite	Early Miocene	4	01	179	66	086	24	270

Note: N: Number of faults used for paloe-stress calculations; pl: plunge; az:azimuth. (1) Ferrari *et al.* (2013).

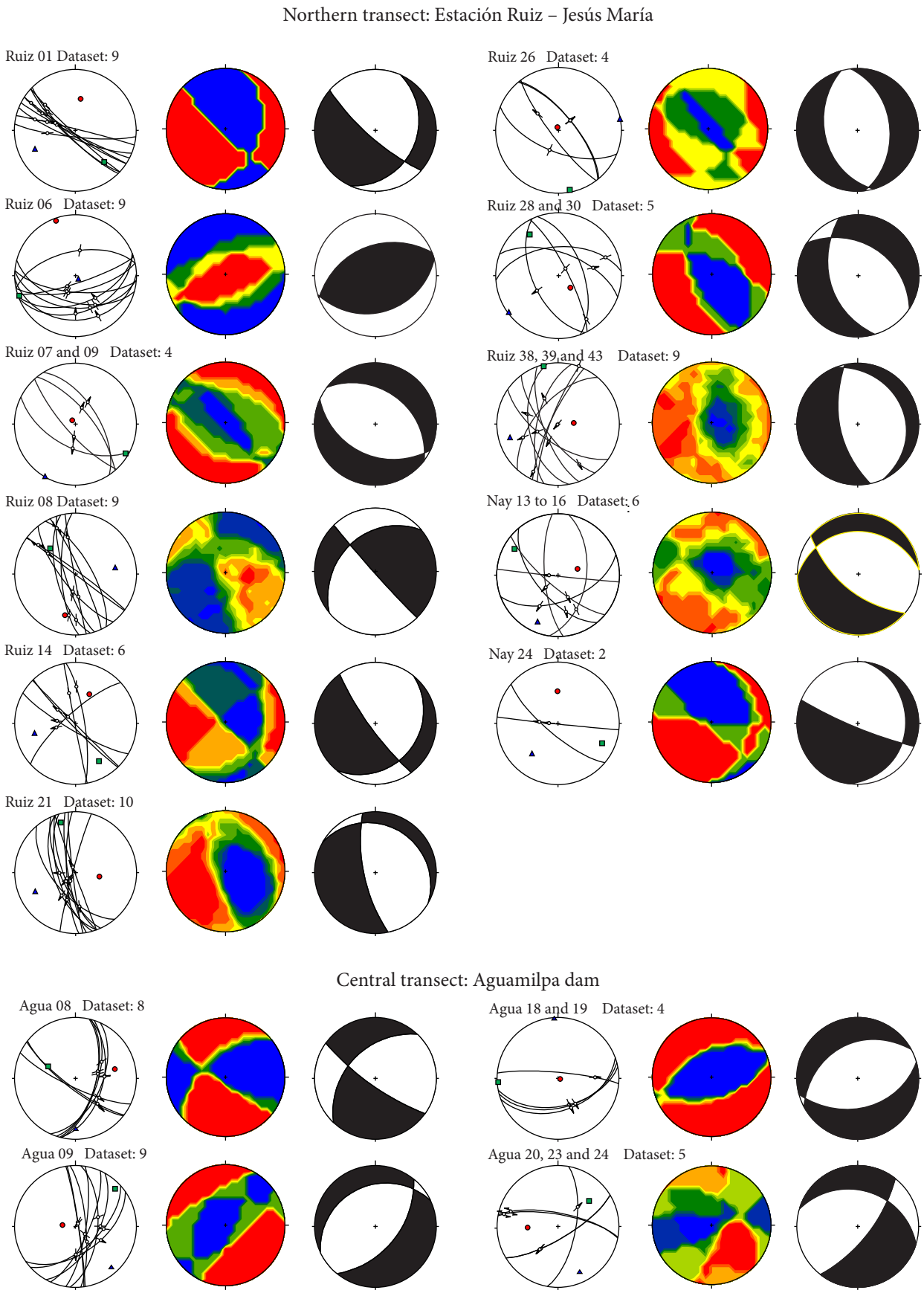

Figure 10. Fault planes with fault-slip data, dihedral density plot and resultant right-dihedra calculations for each structural site shown in Figures 4 to 6.

rupt the continuity of the Pochotitán fault system, which to the south consists of a series NNW-SSE striking west dipping normal faults. To the north, the northern termination of the Pochotitán fault system is slightly rotated counterclockwise and display a minor right-lateral strike-slip component of motion. As a whole, these structures define a complex accommodation zone along which the Santiago river found its way to the coast. The N-S faults observed on this transect are minor normal faults, mostly dipping east, and some of them show a small left-lateral component (Figure 5).

El Cajón Dam-Sierra de Pajaritos transect

Along the El Cajón-Sierra de Pajaritos transect, the dominant faults strike from NNW to NNE (Figure 11c). These faults are primarily normal, with occasionally right lateral strike-slip component (Figure 6). This group of faults is parallel to the main ~N-S structure forming the Huajimic and Camotlán half grabens (Figures 3l, 6 and 7d). The westernmost part of the transect is dominated by the NNW-SSE striking Pochotitán fault system, which tilt early Miocene ignimbrites down to the SWS (Figure 7c). These early Miocene ignimbrites are covered by younger mafic lavas (11 to 10 Ma) of the TMVB (Ferrari *et al.*, 2000b; 2002).

In the eastern part of the transect (Figure 7d), the Sierra de Pajaritos is bounded by two main fault systems: the N-S to NNE-SSW west-dipping faults which form the eastern edge of the Huajimic half graben and the E-W to ENE-WSW faults of El Roble accommodation zone (Figure 6, Figure 11c). These two fault patterns was also observed at outcrop scale. The kinematics of these faults were difficult to establish due to the lack of kinematic indicators. Nevertheless, at site Cam 44 (Figure 6) kinematic indicators corroborate the left lateral strike-slip motion of these faults (Table 1).

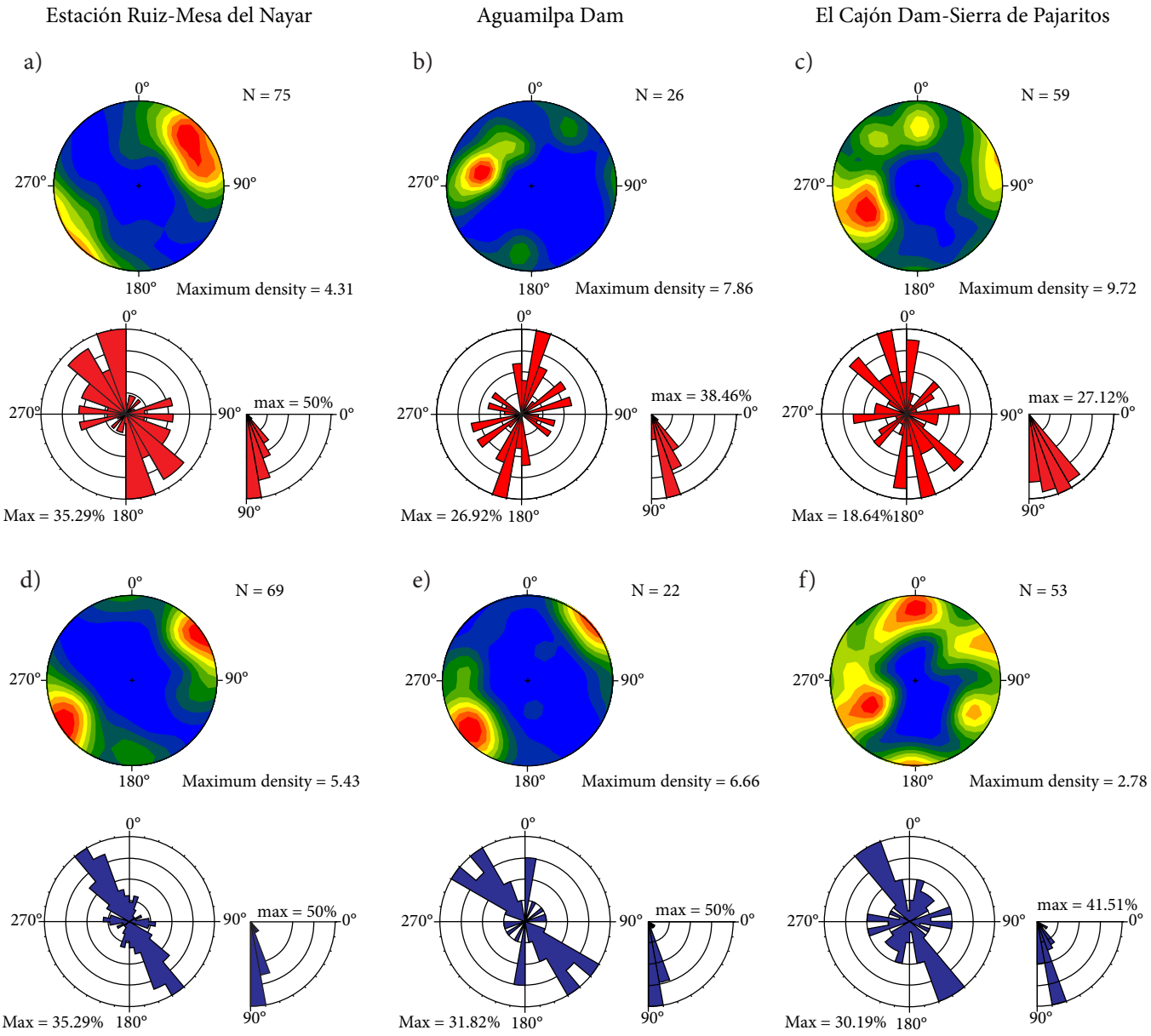

Figure 11. Pole density plot and rose diagram for faults (panels a-c) and dikes (panels d-f) measured in the study area. Diagrams are equal angle projection, lower hemisphere. Rose diagram interval: 20°, dip angle interval: 10°, maximum values represent the percentage of the data grouped in the maximum value.

Mafic dikes

Along the three transects we observed a large number of mafic dikes. The most common dike orientation is NNW-SSE to NW-SE, although other orientations were found locally (Figure 11d-11f). Dike orientation is important to estimate the least principal stress at the time of intrusion, which tends to be normal to the strike of a subvertical dike (Pollard, 1987). We recognized three groups of dike orientations: NNW to NW striking, E-W striking and N-S to NNE-SSW striking.

Dikes striking NW to NNW are by far the most common (Figure 11d–11f). These are mostly located along the western part of the northern and southern transects (Estación Ruiz-Jesús María and El Cajón Dam–Sierra de Pajaritos transects) (Figure 4 and 6). They are also common in the Aguamilpa dam transect (Figure 5). Most of these mafic dikes have subvertical dip (between 80 and 90°) and usually intrude along previously existing normal faults, which commonly remain inactive after intrusion. Only some of the faults show evidence of reactivation, such as fault gouges and striated dike walls (Figure 3d), and at least in one case a dike was observed to be cut by the same fault it intruded (Figure 3e). Several of these dikes have been dated between 11.5 and 11 Ma (Damon *et al.*, 1979; Clark *et al.*, 1981; Soto and Ortega, 1982; Frey *et al.*, 2007).

A second group of dikes, striking E-W and dipping 70-90° (dipping both N and S) was found in the eastern part of the Estación Ruiz-Jesús María transect and, to a lesser extent, in the El Cajón dam-Sierra de Pajaritos transect (Figure 9d and 9f). They cut the lower ignimbrite and volcano-sedimentary sequence and do not seem to have intruded along pre-existing faults. At site Nay 13 an E-W striking dike was observed cutting the ignimbrite sequence and feeding into an overlying basaltic lava flow (Figure 3c).

Some scattered dikes, striking NNE-SSW and NE-SW were also found locally in the Aguamilpa Dam and the El Cajón-Sierra de Pajaritos transects (Figure 11e and 11f). Usually, these dikes are associated with faults observed in these two areas (Figure 11b and 11c).

DISCUSSION

The meso-scale faults observed along the studied transects can be grouped into three sets, and can be associated to the two extensional phases that have occurred since the late Oligocene, defined in Ferrari *et al.* (2013). The dominant fault orientation is ~N-S striking, with subordinate NNW-SSE to NW-SE and ~E-W to NE-SW orientations (Figure 11a–11c).

The N-S fault set corresponds to the major N-S striking structures located in the eastern part of the study areas: the Jesús María, Sierra de Alíca, Sierra de Pajaritos, and Puente de Camotlán half-grabens. The kinematic analysis of these N-S striking faults indicates that they have a dominantly normal motion with a minor strike-slip component. We illustrate the relationship between fault plane dip and the striae plunge contained on each fault plane (Figure 10), which determine the kinematics of the faults (Figure 12). The data from the eastern and western part of the northern and southern transects were plotted separately. Faults measured in the eastern part of these transects (Mesa del Nayar and Sierra de Pajaritos areas) are dominated by pure normal motion and, to a lesser extent, by almost pure strike-slip motion, with very rare oblique slip faults (Figures 12b and 11e). Field relations of dated units show that the activity of the N-S striking faults began during the emplacement of the ~23.5 Ma Las Canoas ignimbrite succession and was complete by ~18 Ma (Ferrari *et al.*, 2013). The direction of the minimum principal stress (σ3) calculated for the ~N-S structures indicate that this deformation phase was characterized by E-W to ENE-WSW crustal stretching (Figure 13).

The second set of faults, characterized by NNW to NW orientations is mostly found in the western part of the transects (Figure 11a-11c) and correspond to the San Pedro-Acaponeta and Pochotitán fault systems. These fault systems defines the western limit of the SMO (Figure 2) and tilt the ignimbrite sequence as much as 35° down to the E-NE. We consider that the activity of these NNW to NW faults began at *ca.* 21

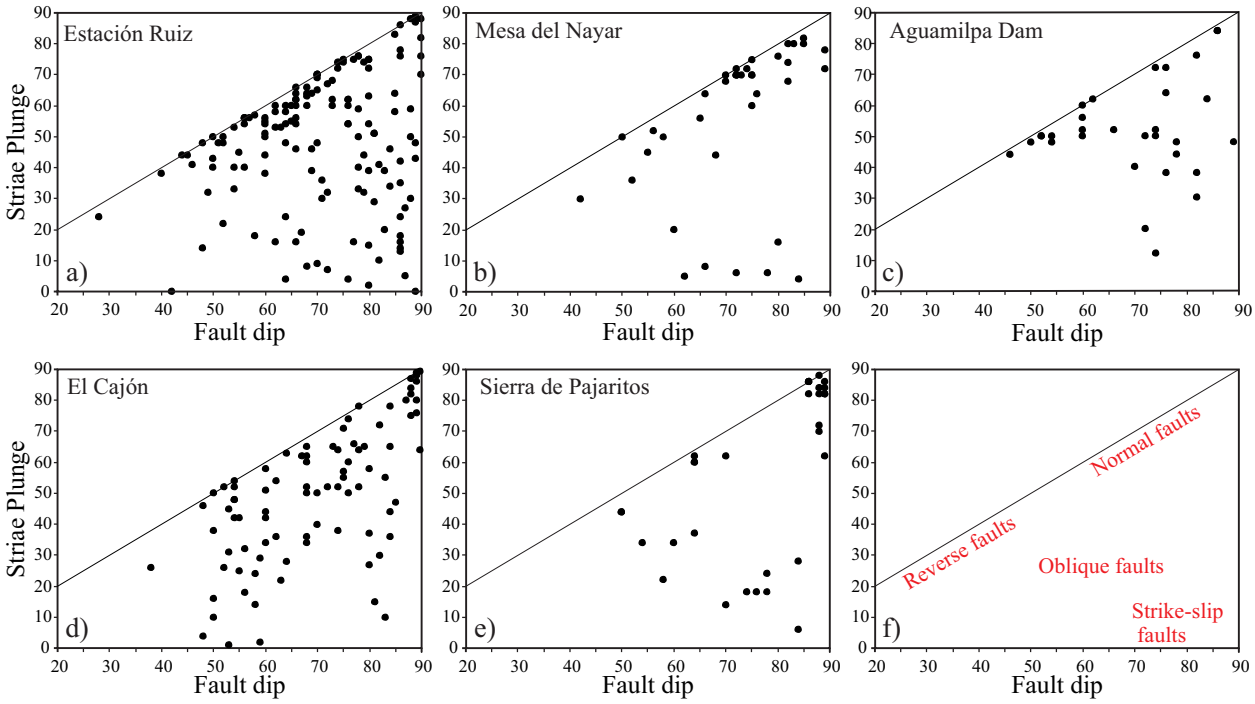

Figure 12. Fault classification diagram based on the fault dip *vs.* striae plunge values, for different zones of the study transects. a) and b), data from Estación Ruiz-Jesús María transect; c), data from Aguamilpa Dam transect; d) and e), from El Cajón-Sierra de Pajaritos transect; f), classification of fault kinematics.

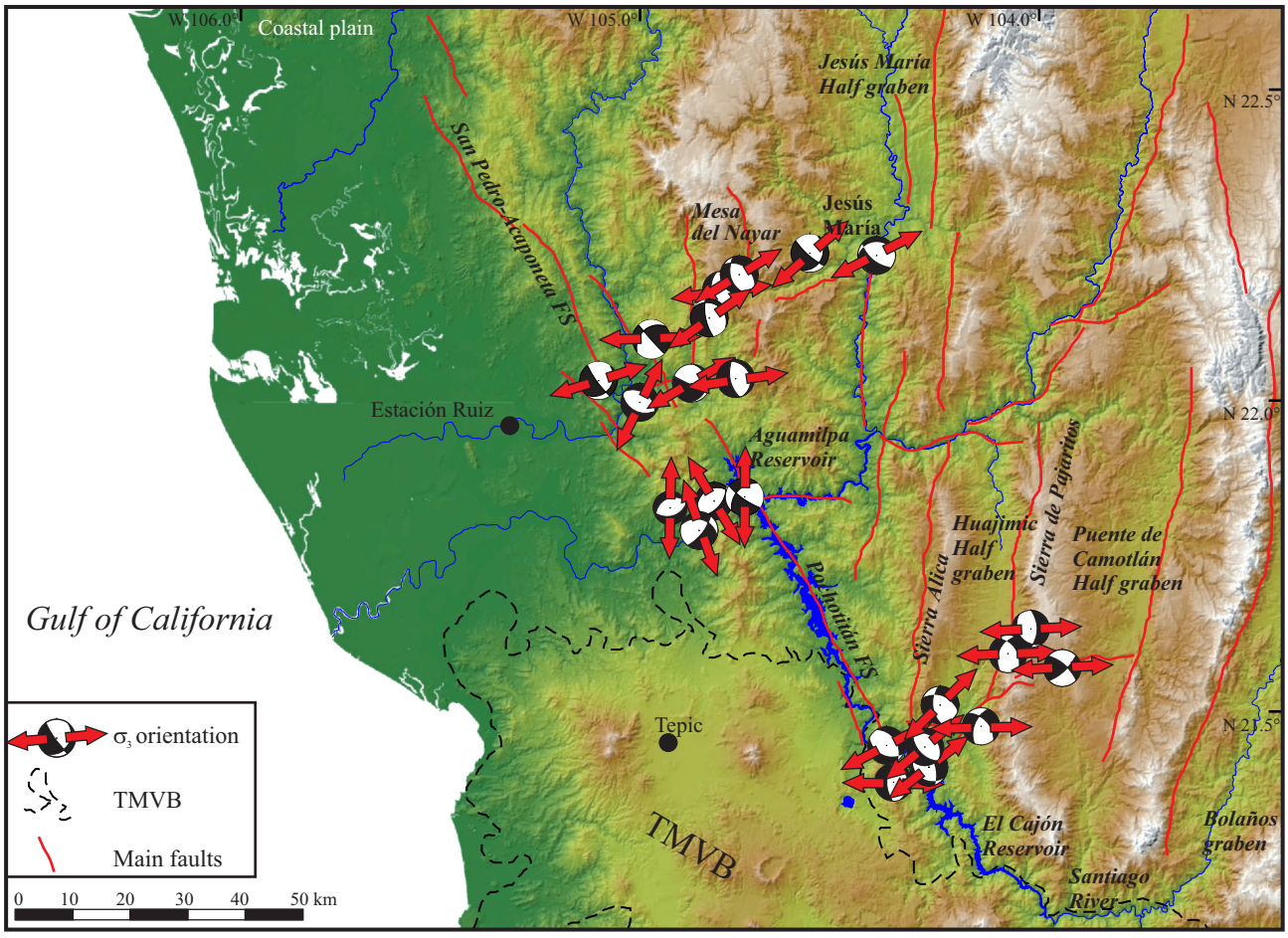

Figure 13. Regional map showing the calculated σ3 orientation at each structural site for which a right-dihedra was calculated.

Ma because they cut the El Nayar ignimbrite sequence and expose some shallow intrusive bodies with ages between *ca.* 20 and 17 Ma (Ferrari *et al.*, 2002; Duque-Trujillo, *et al.*, in press). The minimum age estimate for the activity of these faults is constrained by a series of flat-lying basaltic lavas as old as 10.5 Ma that are found covering the tilted ignimbrites along the coastal plain (Ferrari *et al.*, 2013, and references therein). Several of these faults have a pure normal displacement (Figures 12a, 11c and 11d), with an ENE-WSW orientation of the minimum principal stress (σ3), indicating a slight counterclockwise rotation from the E-W stretching direction determined on the N-S striking faults mapped in the eastern part of the study area (Figure 13). Several faults measured along the San Pedro-Acaponeta and Pochotitán fault system are oblique-slip with a right-lateral strike-slip component (Figure 12a, 12c and 12d). The majority of these faults are found in proximity of accommodation zones (El Naranjo, Aguamilpa, and El Roble; Figures 4, 5, 6) and can be associated to block rotation and/or interaction with transverse structures of these shear zones. Alternatively, if these systems were active at the same time of the ~N-S fault systems, the E-W extension that characterize the early Miocene regime may have induced a right-lateral oblique motion on these NNW striking planes.

The younger group of mafic dikes emplaced along the western SMO, support the dominant extensional kinematics deduced for the San Pedro-Acaponeta and Pochotitán fault systems. These dikes are NNW to NW striking (Figure 11d-11f). Assuming that they were emplaced orthogonal to the former σ3 (Delaney, *et al.*, 1986), they indicate an ENE or NE trending minimum principal stress (σ3) at the time of emplacement. As mentioned before, these dikes were emplaced between 11.5 and 11 Ma, at the end of the period of activity of the San Pedro-Acaponeta and Pochotitán fault systems. Due to the preferred orientation of the San Pedro-Acaponeta and Pochotitán fault systems (NNW to NW), a ENE to NE oriented minimum principal stress would had been expressed with normal kinematic faults along them, instead of right-lateral. This implies that these fault systems had a minimum oblique, right-lateral motion until ca. 11 Ma. This also suggests that if right-lateral transtension began within the Gulf area prior to ~11 Ma (*e.g.*, Fletcher *et al.*, 2007; Sutherland *et al.*, 2012), the southeastern margin of the Gulf was not significantly affected. Such hypothesized dextral transtensional deformation must have occurred further west of our study area, and possibly preserved beneath that coastal plain or the offshore rifted continental shelf. At a regional scale, an initial ~E-W extension was accommodated along N-S striking faults, which then turned into a more ENE extension, accommodated along NNW faults which only affected the westernmost flank of the SMO. Ferrari *et al.* (2013) and Bryan *et al.* (2014) proposed that this tectonic change could have taken place between 21 and 18 Ma, which is now confirmed by the counterclockwise rotation of the minimum principal stress (σ3) determined in this work.

The third set of faults observed strikes E-W, ENE-WSW or NE-SW and have a transverse orientation with respect to the other two sets (Figure 2). Although this kind of structures has already been reported for the southern SMO (Henry and Aranda-Gómez, 2000; Ferrari, *et al.* 2002), they are uncommon. The ~23.01 Ma age for a ~E-W striking

dike found in the Mesa del Nayar-Jesús María area suggest that these faults may be the oldest structures in the study area. However, in other cases these faults appear contemporaneous with the other two sets, which suggest that they represent transfer or accommodation zones, which separate different domains of extension along the western SMO. Transfer zones are mostly formed along a sharp contrast in amount or style of deformation between rift domains (Faulds and Varga, 1998). Nevertheless, the location of these zones could be controlled by the presence of ancient shear zones, as observed in other rifts (*e.g.*, East African Rift and Gulf of Suez, Rosendahl, 1987; Moustafa, 1996). In the study area, the location of these ~E-W to NE-SW structures may be related to pre-existing basement structures, which could have been reactivated during the progressive E-W to WSW-ENE extension that accompanied the initial rifting of the Gulf of California. Indeed, several E-W to NE-SW striking structures affecting the Cretaceous to Paleogene basement have been reported in the SMO (Henry, 1986; Horner and Enriquez, 1999; Horner and Steyrer, 2005). These structures include folds, thrust faults, foliations, tension gashes, shear fractures, and fault zones, which constitute structural weaknesses prone to be reactivated as rift-related accommodation zones (Henry and Aranda-Gómez, 2000; Ferrari, *et al.* 2002). Although some of the ~E-W structures mark a reversal in the tilting direction of the ignimbrites (*e.g.*, El Roble accommodation zone), this is not a rule in the study area (*e.g.*, Aguamilpa and El Naranjo), where some transverse fault zones seem to locally relay the deformation rather than represent a change in the structural style, as defined by Axen (1995) in Baja California. In particular, the El Naranjo (Figure 5) and Aguamilpa (Figure 6) accommodation zones serve as the structural connection across a broad, ~10 km-wide left step between the Pochotitán and San Pedro-Acaponeta fault systems, while block tilting is everywhere down to the E and ENE. In the case of the El Roble fault zone (Figure 6), it separates the extensional structures associated to the Gulf of California with a complex transpressional zone associated with the interaction between the Jalisco block and the southernmost end of the SMO (Ferrari, 1995; Ferrari *et al.*, 2002).

CONCLUDING REMARKS

We have presented the first detailed structural study of the fault systems that affect the southwestern part of the SMO in northern Nayarit, which constrains the kinematics of the initial rifting of the southeastern margin of the Gulf of California rift. Three main families of faults were identified: 1) A group of ~N-S striking faults, associated to the province bounding structure along the western edge of the SMO, with activity bracketed between 24 and 18 Ma; 2) a family of NNW-SSE to NW-SE striking faults associated to the San Pedro-Acaponeta and Pochotitán fault systems in the western part of the SMO, whose activity is constrained between ~21 and 11 Ma; 3) an E-W to ENE-WSW striking group of faults, which seems to be associated to pre-existing basement structures reactivated as accommodation zones during early and middle Miocene rifting phases.

The kinematic analysis and right-dihedra calculation based on the collected fault dataset, the orientation of extension-related dikes, in addition to the age of rocks affected and unaffected by faults allow us to infer that the minimum principal stress ($\sigma 3$) was oriented ~E-W during the early Miocene (24–18 Ma) phase and subsequently rotated slightly counterclockwise to ENE-WSW during the middle Miocene (18–11 Ma) phase. Deformation kinematics indicates a dominant normal faulting and, to a lesser extent, oblique faulting regime along the southeastern SMO. Fault obliquity can be associated to fault interaction in proximity to accommodation zones as observed near the El Roble accommodation zone in Sierra de Pajaritos. Also, some transtensional motion along NNW striking faults during the early Miocene ~E-W extension cannot be excluded. Our data do not support the hypothesis that significant right-lateral transtensional motion was accommodated in the early to middle Miocene (24–11 Ma) in the southeastern margin of the Gulf of California. Rather, these data support the hypothesis that the onset of dextral transtension in the Gulf of California was delayed until the onset of regional dextral oblique motion between the Pacific and North American plates at *ca.* 12.5 Ma (*e.g.*, Stock and Hodges, 1989; Bennett and Oskin, 2014).

ACKNOWLEDGMENTS

The present work was supported by grant CONACYT 82378 (to Ferrari), CONACYT also supported Duque-Trujillo PhD scholarship. We thank I. Loza Aguirre, P. Botero Santa, G. Antillón Mata, M. Michell for discussion and field assistance. C. Ortega, M.A. García are thanked for assistance in U-Pb and Ar-Ar dating, respectively. A.S. Rosas Montoya, V.M. Pérez Arroyo, G. Rendón and L. Gradilla helped with Ar-Ar sample preparation. Reviews by Scott Bennett, an anonymous reviewer and associated editor Angel Nieto Samaniego greatly helped to improve the quality of the manuscript. T. Orozco-Esquivel is thanked for thoroughly reviewing the final version of the paper.

APPENDIX A. SUPPLEMENTARY MATERIAL

Supplementary files 1 and 2 can be found at the journal web site <http://rmcg.unam.mx/>, in the table of contents of this issue.

REFERENCES

Angelier, J., 1979, Determination of the mean principal directions of stresses for a given fault population: Tectonophysics, 56(3), T17-T26.

Angelier, J., 1984, Tectonic analysis of fault slip data sets: Journal of Geophysical Research, Solid Earth, 89(B7), 5835-5848.

Angelier, J., 1994, Fault slip analysis and palaeostress reconstruction, *in* Hancock, L. (ed.), Continental deformation: Oxford, UK, Pergamon Press, 53-100.

Atwater, T., Stock, J., 1998, Pacific-North America plate tectonics of the Neogene southwestern United States: An update: International Geology Review, 40, 375-402.

Axen, G., 1995, Extensional segmentation of the Main Gulf Escarpment, Mexico and United States: Geology, 23, 515-518, doi:10.1130/0091-7613(1995)023<0515:ESOTMG>2.3.CO;2.

Bennett, S.E., Oskin, M.E., 2014, Oblique rifting ruptures continents: Example from the Gulf of California shear zone: Geology, 42(3), 215-218.

Bennett, S.E.K., Oskin, M.E., Iriondo, A., 2013, Transtensional rifting in the proto-Gulf of California near Bahia Kino, Sonora, Mexico: Geological Society of America Bulletin, 125(11-12), 1752-1782. doi:10.1130/B30676.1

Bonner, J.L., Herrin, E.T., 1999, Surface wave studies of the Sierra Madre Occidental of northern Mexico: Bulletin of the Seismological Society of America, 89(5), 1323-1337.

Bryan, S.E., Ferrari L., 2013, Large igneous provinces and silicic large igneous provinces: Progress in our understanding over the last 25 years: Geological Society of America Bulletin, 125(7/8), 1053-1078, doi: 10.1130/B30820.1.

Bryan, S.E., Ferrari, L., Reiners, P.W., Allen, C.M., Petrone, C.M., Ramos-Rosique, A., Campbell, I.H., 2008, New insights into crustal contributions to large volume rhyolite generation at the mid-Tertiary Sierra Madre Occidental Province, Mexico, revealed by U/Pb geochronology: Journal of Petrology, 49(1), 47-77.

Bryan, S.E., Orozco-Esquivel, T., Ferrari, L., López-Martínez, M., 2014, Pulling apart the Mid to Late Cenozoic magmatic record of the Gulf of California: Is there a Comondú arc?, *in* Gómez-Tuena, A., Straub, S.M., Zellmer,

G.F. (eds.), Orogenic Andesites and Crustal Growth: Geological Society, London, Special Publication 385, 389-407, doi:10.1144/SP385.8

Clark, K.F., Damon, P. E., Shafiquillah, M., Ponce, B.F. Cárdenas, D., 1981, Sección geológica-estructural a través de la parte sur de la Sierra Madre Occidental, entre Fresnillo y la costa de Nayarit: Asociación de Ingenieros Mineros, Metalúrgicos y Geólogos de México, Memoria Técnica XIV, 69-99.

Couch, R.W., Ness, G.E., Sanchez-Zamora, O., Calderón-Riveroll, G., Doguin, P., Plawman, T., Coperude, S., Huehn, B., Gumma, W., 1991, Gravity anomalies and crustal structure of the Gulf and Peninsular Province of the Californias, *in* Dauphin, J.P., Simoneit, B.R.T. (eds), The Gulf and the Peninsular Province of the Californias: American Association of Petroleum Geologists, Memoir 47, 25-45.

Damon, P.E., Nieto-Obregón, J., Delgado-Argote, L., 1979, Un plegamiento neogénico en Nayarit y Jalisco y evolución geomórfica del Río Grande de Santiago: Asociación de Ingenieros Mineros, Metalúrgicos y Geólogos de México, Memoria Técnica, XIII, 156-191.

Delaney, P., Pollard, D., Ziony, J., McKee, E., 1986, Field relations between dikes and joints: Emplacement processes and paleostress analysis: Journal of Geophysical Research, 9., 4920-4938.

Drake, W.R, 2005, Structural analysis, stratigraphy, and geochronology of the San José Island accommodation zone, Baja California Sur, Mexico: Northern Arizona University, M. Sc. Thesis, 271 pp.

Duque-Trujillo, J., Ferrari, L., Orozco-Esquivel, T., López-Martinez, M., Lonsdale, P., Bryan, S., Kluesner, J., Piñero-Lajas, D., Solari, L., in press, Timing of rifting in the Southern Gulf of California and its conjugate margins: insights from the plutonic record: Geological Society of America Bulletin.

Faulds, J.E., Varga, R.J.,1998, The role of accommodation zones and transfer zones in the regional segmentation of extended terranes: Geological Society of America, Special Paper 323, 1-45.

Ferrari, L., 1995, Miocene shearing along the northern boundary of the Jalisco block and the opening of the southern Gulf of California: Geology, 23, 751–754, doi:10.1130/0091-7613(1995)023<0751:MSATNB>2.3.CO;2.

Ferrari, L., Pasquaré, G., Venegas-Salgado, S., Romero-Rios, F., 2000a, Geology of the western Mexican Volcanic Belt and adjacent Sierra Madre Occidental and Jalisco block: Geological Society of America Special Paper, 334, 65-84.

Ferrari, L., Conticelli, S., Vaggelli, G., Petrone, C., Manetti, P., 2000b, Late Miocene mafic volcanism and intraarc tectonics during the early development of the Trans-Mexican Volcanic Belt: Tectonophysics, 318, 161-185.

Ferrari, L., López-Martínez, M., Rosas-Elguera, J., 2002, Ignimbrite flare-up and deformation in the southern Sierra Madre Occidental, western Mexico-implications for the late subduction history of the Farallón Plate: Tectonics, 21(4), doi: 10.1029/2001TC001302.

Ferrari, L., Valencia-Moreno, M., Bryan, S.E, 2007, Magmatism and tectonics of the Sierra Madre Occidental and its relation with the evolution of the western margin of North America, *in* Alaniz-Álvarez, S.A., Nieto-Samaniego, A.F. (eds.), Geology of México: Celebrating the Centenary of the Geological Society of México: Geological Society of America, Special Paper 422, 1-39, doi: 10.1130/2007.2422(01).

Ferrari, L., López-Martínez, M., Orozco-Esquivel, T., Bryan, S.E, Duque-Trujillo, J., Lonsdale, P.F., 2013, Late Oligocene to middle Miocene rifting and syn-extensional magmatism in the southwestern Sierra Madre Occidental, Mexico: the beginning of the Gulf of California rift: Geosphere, 9(5), 1-40.

Fletcher, J.M., Grove, M., Kimbrough, D., Lovera, O., Gehrels, G.E., 2007, Ridge-trench interactions and the Neogene tectonic evolution of the Magdalena Shelf and southern Gulf of California; insights from detrital zircon U/Pb ages from the Magdalena Fan and adjacent areas: Geological Society of America Bulletin, 119(11-12), 1313-1336, doi: 10.1130/ B26067.1.

Frey, H.M., Lange, R.A., Hall, C.M., Delgado Granados, H., Carmichael, I.S.E., 2007, A Pliocene ignimbrite flare-up along the Tepic-Zacoalco rift: Evidence for the initial stages of rifting between the Jalisco block (Mexico) and North America: Geological Society of America Bulletin, 119, 49-64, doi:10.1130/B25950.1.

Gans, P.B., 1997, Large magnitude Oligo-Miocene extension in southern Sonora: Implications for the tectonic evolution of northwest Mexico: Tectonics, 16(3), 388-408.

González-León, C.M., McIntosh, W.C., Lozano-Santacruz, R., Valencia-Moreno, M., Amaya-Martínez, R., Rodríguez-Castañeda, J.L., 2000, Cretaceous and Tertiary sedimentary, magmatic, and tectonic evolution of north-central Sonora (Arizpe and Bacanuchi Quadrangles), northwest Mexico: Geological Society of America Bulletin, 112, 600-610.

Henry, C.D., 1986, East-Northeast-trending structures in western Mexico: evidence for oblique convergence in the late Mesozoic: Geology, 14, 314-317.

Henry, C.D., Aranda-Gómez, J.J., 2000, Plate interactions control middle-late Miocene, proto-Gulf and Basin and Range extension in the southern Basin and Range: Tectonophysics, 318(1), 1-26.

Horner, J. T., Enriquez, E., 1999, Epithermal precious metal mineralization in a strike-slip corridor; the San Dimas District, Durango, Mexico: Economic Geology, 94(8), 1375-1380.

Horner, J.T., Steyrer, H.P., 2005, An analogue model of a crustal-scale fracture zone in West-Central Mexico: Evidence for a possible control of ore forming processes. Neues Jahrbuch fur Geologie und Palaontologie-Abhandlungen, 236(3), 185-206.

Karig, D. E., Jensky, W., 1972, The proto-Gulf of California: Earth and Planetary Science Letters, 17(1), 169-174.

Lizarralde, D., Axen, G.J., Brown, H.E., Fletcher, J.M., González-Fernández, A., Harding, A.J., Holbrook, W.S., Kent, G.M., Paramo, P., Sutherland, F., Umhoefer, P.J., 2007, Variable styles of rifting in the Gulf of California: Nature, 448, 466-469, doi:10.1038/nature06035.

McDowell, F.W., Keizer, R.P., 1977, Timing of mid-Tertiary volcanism in the Sierra Madre Occidental between Durango City and Mazatlán, Mexico: Geological Society of America Bulletin, 88(10), 1479–1487.

McDowell, F.W., Clabaugh, S.E., 1979, Ignimbrites of the Sierra Madre Occidental and their relation to the tectonic history of western Mexico: Geological Society of America, Special Paper 180, 113-124.

McDowell, F.W., McIntosh, W.C., 2012, Timing of intense magmatic episodes in the northern and central Sierra Madre Occidental, western Mexico: Geosphere, 8, 1505–1526, doi:10.1130/GES00792.1.

McDowell, F.W, Roldán-Quintana, J., Amaya-Martínez, R., 1997, Interrelationship of sedimentary and volcanic deposits associated with Tertiary extension in Sonora, Mexico: Geological Society of America Bulletin, 109(10), 1349-1360.

Moustafa, A. R., 1996, Internal structure and deformation of an accommodation zone in the northern part of the Suez rift: Journal of Structural Geology, 18, 93-108.

Murray, B.P., Busby, C.J., Ferrari, L., Solari, L.A., 2013, Synvolcanic crustal extension during the mid-Cenozoic ignimbrite flare-up in the northern Sierra Madre Occidental, Mexico: Evidence from the Guazapares Mining District region, western Chihuahua: Geosphere, 9, doi:10.1130/GES00862.1.

Nieto-Obregón, J., Delgado-Argote, L., Damon, P.E., 1981, Relaciones petrológicas y geocronológicas del magmatismo de la Sierra Madre Occidental y el Eje Neovolcánico en Nayarit, Jalisco y Zacatecas: Asociación de Ingenieros Mineros, Metalúrgicos y Geólogos de México, Memoria Técnica XIV, 327-361.

Nourse, J., Anderson, T., Silver, L., 1994, Tertiary metamorphic core complexes in Sonora, Northwestern Mexico: Tectonics, 13(5), 1161-1182.

Ortner, H., Reiter, F., Acs, P., 2002, Easy handling of tectonic data: the programs TectonicVB for Mac and TectonicsFP for Windows™: Computers & Geosciences, 28(10), 1193-1200.

Persaud, P., Pérez-Campos, X., Clayton, R.W., 2007, Crustal thickness variations in the margins of the Gulf of California from receiver functions: Geophysical Journal International, 170(2), 687-699.

Pollard, D.D., 1987, Elementary fracture mechanics applied to the structural interpretation of dykes, *in* Halls H.C., Fahrig W.F. (eds.), Mafic dyke swarms: Geological Association of Canada, Special Paper 34, 5-24.

Ramos-Rosique, A., 2013, Timing and evolution of Late Oligocene to Early Miocene magmatism and epithermal mineralization in the central Bolaños Graben, southern Sierra Madre Occidental, México: London, UK, Kingston University, Ph.D. thesis, 215 pp.

Righter, K., Carmichael, I.S.E., Becker, T., 1995, Pliocene-Quaternary faulting and volcanism at the intersection of the Gulf of California and the Mexican Volcanic Belt: Geological Society of America Bulletin, 107, 612-626.

Rodríguez-Castañeda, J.L., Rodríguez-Torres, R., 1992, Geología estructural y estratigrafía del área entre Guadalajara y Tepic, Estados de Jalisco y

Nayarit, México: Revista del Instituto de Geología UNAM, 10, 99-110.
Rosendahl, B.R., 1987, Architecture of continental rifts with special reference to East Africa: Annual Review of Earth and Planetary Science Letters, 15, 445-504.
Rossotti, A., Ferrari, L., López-Martinez, M., Rosas-Elguera, J., 2002, Geology of the boundary between the Sierra Madre Occidental and the Trans-Mexican Volcanic Belt in the Guadalajara region, western Mexico: Revista Mexicana de Ciencias Geológicas, 19, 1-15.
Savage, B., Wang, Y., 2012, Integrated model of the crustal structure in the Gulf of California Extensional Province: Bulletin of the Seismological Society of America, 102(2), 878-885.
Sawlan, M.G., Smith, J.G., 1984, Petrologic characteristics, age and tectonic setting of Neogene volcanic rocks in northern Baja California Sur, Mexico, *in* Frizzell, V.A. (ed.), Geology of the Baja California Peninsula: Society of Economic Paleontologists and Mineralogists, Pacific Section, 39, 237-251.
Scheubel, F.R., Clark, K.F., Porter, E.W., 1988, Geology, tectonic environment and structural controls in the San Martin de Bolaños district, Jalisco, Mexico: Economic Geology, 83, 1703-1720.
SGM (Servicio Geológico Mexicano), 1996, Carta Geológico-Minera Santa María del Oro F13-D32, Nayarit, scale 1:50.000: Pachuca, Mexico, Servicio Geológico Mexicano, 1 map.
SGM (Servicio Geológico Mexicano), 1998, Carta Geológico-Minera Tepic F13-8, Nayarit y Jalisco, scale 1:250.000: Pachuca, Mexico, Servicio Geológico Mexicano, 1 map.
SGM (Servicio Geológico Mexicano), 1999, Carta Geológico-Minera Escuinapa F13-5, Nayarit y Jalisco, scale 1:250.000: Pachuca, Mexico, Servicio Geológico Mexicano, 1 map.
SGM (Servicio Geológico Mexicano), 2006, Carta Geológico-Minera El Venado F13-D11, Nayarit y Jalisco, scale 1:50.000: Pachuca, Mexico, Servicio Geológico Mexicano, 1 map.
Soto, M.A., Ortega J.G., 1982, Geología del Río Santiago en los estados de Jalisco y Nayarit, México: México City, XII Convención de la Sociedad Geológica Mexicana, Memoria, 20 pp.
Stewart, J., 1998, Regional characteristics, tilt domains, and extensional history of the later Cenozoic Basin and Range Province, western North America, *in* Faulds, J. E., Stewart, J. H. (eds.), Accommodation Zones and Transfer Zones: The Regional Segmentation of the Basin and Range Province: Geological Society of America, Special Paper, 323, 47-74,
Stock, J.M., Hodges, K.V., 1989, Pre-Pliocene extension around the Gulf of California and the transfer of Baja California to the Pacific plate: Tectonics, 8(1), 99-115.
Sutherland, F.H., Kent, G.M., Harding, A.J., Umhoefer, P.J., Driscoll, N.W., Lizarralde, D., Fletcher, J.M., Axen, G.J., Holbrook, W.S., González-Fernández, A., Lonsdale, P., 2012, Middle Miocene to early Pliocene oblique extension in the southern Gulf of California: Geosphere, 8, 752-770, doi:10.1130/GES00770.1.
Swanson, E.R., Kempter, K.A., McDowell, F.W., McIntosh, W.C., 2006, Major ignimbrites and volcanic centers of the Copper Canyon area: A view into the core of Mexico's Sierra Madre Occidental: Geosphere, 2(3), 125-141.
Umhoefer, P.J., 2011, Why did the Southern Gulf of California rupture so rapidly?—Oblique divergence across hot, weak lithosphere along a tectonically active margin: GSA Today, 21(11), 1-10.
Umhoefer, P., Dorsey, R., Willsey, S., Mayer, L., Renne, P., 2001, Stratigraphy and geochronology of the Comundú Group near Loreto, Baja California Sur, Mexico: Sedimentary Geology, 144(1), 125-147.
Vega-Granillo, R., Calmus, T., 2003, Mazatán metamorphic core complex (Sonora, Mexico): structures along the detachment fault and its exhumation evolution: Journal of South American Earth Sciences, 16(4), 193-204.
Wong, M.S., Gans, P.B., Scheier, J., 2010, The $^{40}Ar/^{39}Ar$ thermochronology of core complexes and other basement rocks in Sonora, Mexico: Implications for Cenozoic tectonic evolution of northwestern Mexico: Journal of Geophysical Research, 115(B7), doi: 10.1029/2009JB007032.

Manuscript received: April 9, 2014
Corrected manuscript received: September 22, 2014
Manuscript accepted: September 26, 2014